

# Chorismate-Utilizing Enzymes Isochorismate Synthase, Anthranilate Synthase, and *p*-Aminobenzoate Synthase: Mechanistic Insight through Inhibitor Design

Marisa C. Kozlowski, Norma J. Tom, Christopher T. Seto, Andrea M. Sefler, and Paul A. Bartlett\*

Contribution from the Department of Chemistry, University of California, Berkeley, California 94720-1460

Received July 11, 1994<sup>⊗</sup>

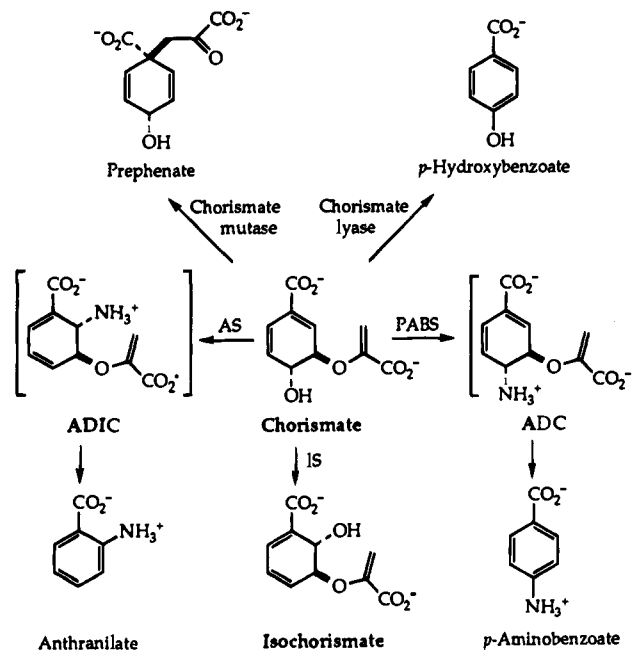
**Abstract:** Three enzymes of the shikimic acid pathway, isochorismate synthase (IS), anthranilate synthase (AS), and *p*-aminobenzoate synthase (PABS), exhibit significant sequence homology and may be related mechanistically. Compounds **1**, **2**, and **3** were designed to mimic, in their all-axial conformations, the putative transition state for these enzymes. The inhibitors were prepared in racemic form starting from Diels–Alder addition of a propiolate ester to a protected 1-oxy- or 1-amino-1,3-butadiene in 14%, 4%, and 9% overall yields, respectively. All three compounds are competitive inhibitors of the three enzymes, binding IS and AS strongly and PABS weakly. For both IS and AS, the affinity of the 6-amino-4-hydroxy isomer **2** is ca. 10-fold that of the 4-amino-6-hydroxy isomer **3**, a difference that is largely due to their conformational equilibria; **2** is 25 ± 2% axial and **3** is 6 ± 3% axial, as determined by the temperature dependence of their NMR spectra. The similarity between IS and AS was extended by the finding that IS, like AS, catalyzes formation of 2-amino-2-deoxyisochorismate (ADIC) in the presence of ammonia. These observations are consistent with direct 1,5-substitution mechanisms for both IS and AS; the weak inhibition of PABS by these inhibitors suggests that it operates by a significantly different mechanism.

## Introduction

**Background.** The shikimate–chorismate manifold possesses a variety of unique and mechanistically interesting transformations which have been extensively reviewed.<sup>1–7</sup> This pathway has generated considerable interest because it is unique to plants and microorganisms and thus is an attractive target for potential herbicides or antibiotics. The branch-point metabolite chorismate is a precursor to a large number of aromatic metabolites, including the aromatic amino acids, many of the quinones, and the folic acids. Chorismate is subject to five distinct transformations (Scheme 1); those catalyzed by isochorismate synthase (IS), anthranilate synthase (AS), and *p*-aminobenzoate synthase (PABS) display certain mechanistic and enzymatic similarities and are the focus of this report.

IS, AS, and PABS all require magnesium for activity and catalyze apparently similar reactions; moreover, they are related at the genetic level. IS is a monomeric 43-kDa protein encoded by the *entC* gene in *Escherichia coli*. AS from several sources consists of two components, encoded by the *trpE* and *trpG* genes, respectively. The counterpart to IS is the 50-kDa AS-I subunit which contains the chorismate binding site and catalyzes both the formation of 2-amino-2-deoxyisochorismate (ADIC) and its elimination to anthranilate; the 20-kDa AS-II subunit is a glutamine amidotransferase that provides the ammonia. PABS from *E. coli* is a three protein complex, the *pabB*, *pabA*, and *pabC* gene products. The 50-kDa PABS-I unit converts

Scheme 1



chorismate and ammonia into 4-amino-4-deoxychorismate (ADC), and the 20-kDa PABS-II is the glutamine amidotransferase. In this case, there is a separate aromatizing enzyme, the 30-kDa aminodeoxychorismate lyase, PABS-III.

The chorismate binding proteins of these enzyme systems (IS, AS-I, and PABS-I) are of comparable size and exhibit significant sequence similarity, especially in the carboxy terminal portions, which are suggested to contain the active sites.<sup>8–10</sup> In addition, antibodies raised against AS-I cross-react

<sup>⊗</sup> Abstract published in *Advance ACS Abstracts*, January 15, 1995.

(1) Ganem, B. *Tetrahedron* **1978**, *34*, 3353–3383.

(2) Weiss, U.; Edwards, J. M. *The Biosynthesis of Aromatic Compounds*; Wiley-Interscience: New York, 1987; pp 260–270.

(3) Walsh, C. T.; Liu, J.; Rusnak, F.; Sakaitani, M. *Chem. Rev.* **1990**, *90*, 1105–1129.

(4) Dewick, P. M. *Nat. Prod. Rep.* **1988**, *5*, 73–97.

(5) Bentley, R. *Crit. Rev. Biochem. Mol. Biol.* **1990**, *25*, 307–384.

(6) Poulsen, C.; Verpoorte, R. *Phytochemistry* **1991**, *30*, 377–386.

(7) Haslam, E. *Shikimic Acid Metabolism and Metabolites*; Wiley: New York, 1993.

(8) Goncharoff, P.; Nichols, B. P. *J. Bacteriol.* **1984**, *159*, 57–62.

(9) Goncharoff, P.; Nichols, B. P. *Mol. Biol. Evol.* **1988**, *5*, 531–548.

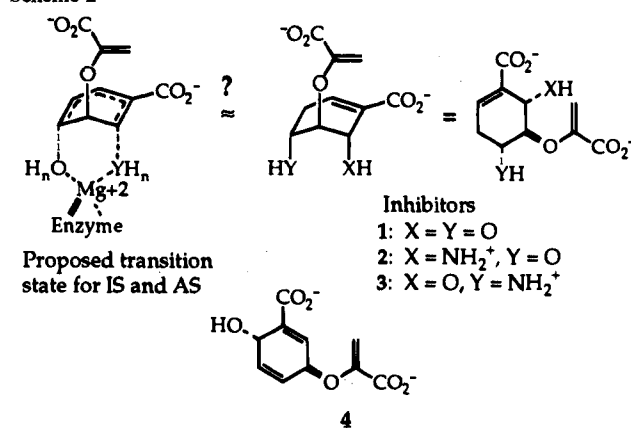
with PABS-I. The structural similarity of these enzymes may reflect their ability to bind chorismate; however, chorismate mutase and chorismate lyase also utilize chorismate as a substrate, but they are not similar in sequence.<sup>5,11,12</sup> It is more likely that the IS, AS, and PABS chorismate-binding subunits are related evolutionarily and arose from a common ancestor.

Both IS and AS-I catalyze an unusual 1,5-substitution reaction. In the isomerization of chorismate to isochorismate (Scheme 1), <sup>18</sup>O labeling studies have shown that the incoming hydroxyl is derived from solvent and not via intramolecular transfer.<sup>13,14</sup> The reaction is reversible with a  $K_{eq} = 0.56$  favoring chorismate. The initial reaction catalyzed by AS-I is very similar to that of IS, except that the incoming nucleophile is ammonia. The immediate product of the substitution, ADIC, has been prepared by independent synthesis and found to be a viable substrate for the enzyme.<sup>15,16</sup> Morollo et al. have recently isolated and characterized ADIC as it accumulates in an *E. coli* mutant and shown that its formation is reversible ( $K \approx 4$  favoring ADIC), but much slower than the elimination step.<sup>17,18</sup> The last step catalyzed by AS-I, elimination of the enolpyruvyl side chain of ADIC to generate anthranilate, has no counterpart in the IS-catalyzed transformation.

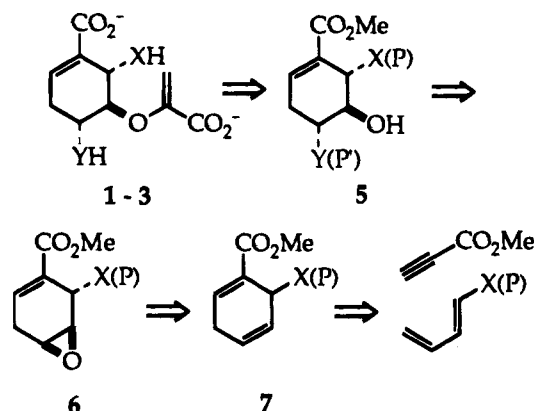
The first step in the PABS-catalyzed sequence is substitution of the 4-hydroxyl group of chorismate with ammonia; however, in this case, it occurs with overall retention of position and stereochemistry. This intermediate ADC has also been synthesized and shown to be a competent substrate for PABS.<sup>19</sup> Anderson et al. have observed the formation of ADC during enzyme turnover and found that the reaction is reversible ( $K_{eq} = 6.1$  favoring ADC).<sup>20</sup> In this case, the elimination of pyruvate to generate *p*-aminobenzoate is catalyzed by a separate protein, PABS-III.<sup>12,21,22</sup>

**Inhibitor Design.** Several lines of evidence led to the suggestion of a magnesium-coordinated transition state for the conversion of chorismate to isochorismate and, by analogy, to ADIC (Scheme 2).<sup>3</sup> Magnesium is required for IS activity, and NMR and EPR measurements indicate that magnesium interacts with chorismate at the active site of AS.<sup>23</sup> Kinetic data also reveal a synergism in the binding of magnesium and chorismate to AS. How PABS catalyzes the direct substitution of the chorismate OH, with retention of configuration, is less apparent. The observation that isochorismate is not an alternative substrate argues against sequential 1,5-substitutions: chorismate  $\rightarrow$  isochorismate  $\rightarrow$  ADC.<sup>19,24</sup> The alternative sequence of 1,3-substitutions, via **4**, has been addressed by Ganem et al. through

Scheme 2



Scheme 3



the synthesis of this species; unfortunately, its instability precluded their evaluation of its enzymatic behavior and its role remains unresolved.<sup>25</sup>

The bisubstrate analogs **1–3** were designed to mimic the putative transition states for IS and AS and to serve as mechanistic probes of the three enzymes. In addition to their potential as transition state analogs, these compounds were expected to act as selective inhibitors, based on their substitution patterns: diol **1** was predicted to inhibit IS preferentially, compound **2**, AS, and compound **3**, PABS, to the extent that PABS shares a similar mechanism. Interestingly, this pattern of selectivity was not observed, leading us to reexamine our assumptions regarding the mechanisms and specificities of the enzymes.

## Results

**Synthetic Plan.** Our initial approach to the inhibitors involved introduction of the double bond late in the sequence, by elimination of a sulfoxide or sulfone from C-2. This approach proved troublesome, so a strategy was developed in which the double bond was maintained throughout the synthesis (Scheme 3). A suitably protected, trisubstituted analog, **5**, was required for selective incorporation of the enolpyruvyl side chain; this species could be obtained from nucleophilic opening of epoxide **6**, which would arise from selective oxidation of cyclohexadiene **7**. These dienes were available from Diels–Alder condensation of a propiolate ester and a substituted butadiene. The key problem anticipated in this synthetic scheme lay in selective opening of the epoxide moieties.

(10) Ozenberger, B. A.; Brickman, T. J.; McIntosh, M. A. *J. Bacteriol.* **1989**, *171*, 775–783.

(11) Hudson, G. S.; Davidson, B. E. *J. Mol. Biol.* **1984**, *180*, 1023–51.

(12) Nichols, B. P.; Siebold, A. M.; Doktor, S. Z. *J. Biol. Chem.* **1989**, *264*, 8597–8601.

(13) Liu, J.; Quinn, N.; Berchtold, G. A.; Walsh, C. T. *Biochemistry* **1990**, *29*, 1417–1425.

(14) Gould, S. J.; Eisenberg, R. L. *Tetrahedron* **1991**, *47*, 5979–5990.

(15) Teng, C.-Y. P.; Ganem, B. *J. Am. Chem. Soc.* **1984**, *106*, 2463–2464.

(16) Policastro, P. P.; Au, K. G.; Walsh, C. T.; Berchtold, G. A. *J. Am. Chem. Soc.* **1984**, *106*, 2443–2444.

(17) Morollo, A. A.; Bauerle, R. *Proc. Nat. Acad. Sci. U.S.A.* **1993**, *90*, 9983–9987.

(18) Morollo, A. M.; Finn, M. G.; Bauerle, R. *J. Am. Chem. Soc.* **1993**, *115*, 816–817.

(19) Teng, C.-Y. P.; Ganem, B.; Doktor, S. Z.; Nichols, B. P.; Bhatnagar, R. K.; Vining, L. C. *J. Am. Chem. Soc.* **1985**, *107*, 5008–5009.

(20) Anderson, K. S.; Kati, W. M.; Ye, Q.-Z.; Liu, J.; Walsh, C. T.; Benesi, A. J.; Johnson, K. A. *J. Am. Chem. Soc.* **1991**, *113*, 3198–3200.

(21) Ye, Q.-Z.; Liu, J.; Walsh, C. T. *Proc. Nat. Acad. Sci. U.S.A.* **1990**, *87*, 9391–9395.

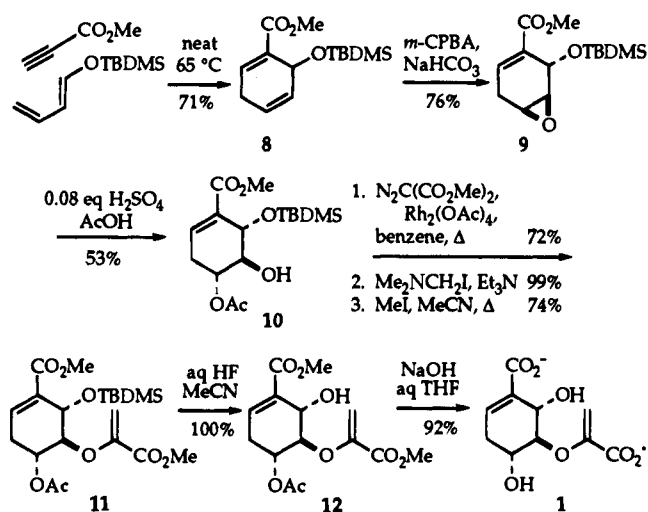
(22) Green, J. M.; Nichols, B. P. *J. Biol. Chem.* **1991**, *266*, 12971–12975.

(23) Summerfield, A. E.; Bauerle, R.; Grisham, C. M. *J. Biol. Chem.* **1988**, *263*, 18793–18801.

(24) Johanni, M.; Hofmann, P.; Leistner, E. *Arch. Biochem. Biophys.* **1989**, *271*, 495–501.

(25) Mattia, K. M.; Ganem, B. *J. Org. Chem.* **1994**, *59*, 720–728.

Scheme 4

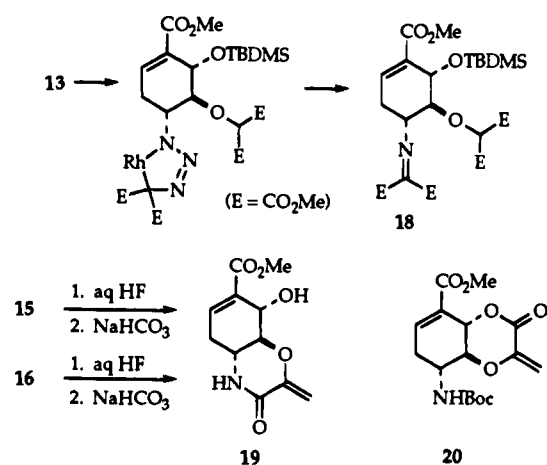
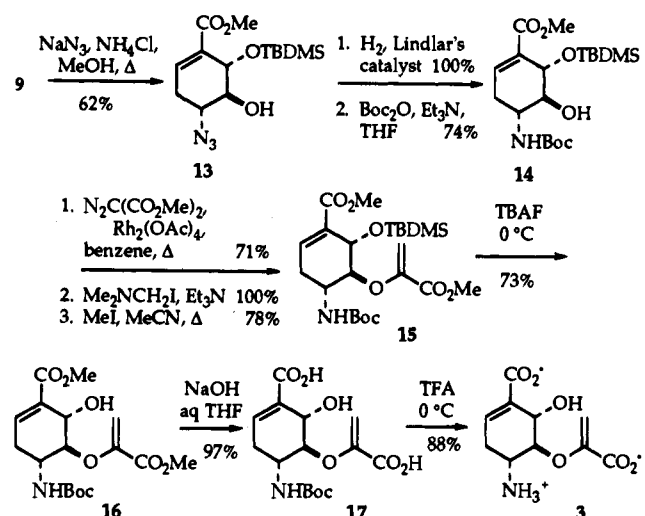


**Synthesis of Diol 1.**<sup>26</sup> Diels–Alder reaction of methyl propiolate with 1-(*tert*-butyldimethylsilyloxy)-1,3-butadiene using a procedure modified from that reported<sup>27</sup> generates cyclohexadiene **8** in good yield (Scheme 4). Epoxide **9** is synthesized by oxidation of the more electron-rich double bond *trans* to the bulky silyl ether. Opening of this epoxide by acetolysis indeed proved difficult. No reaction was obtained using  $\text{Al}_2\text{O}_3$ <sup>28</sup> or 2,3-dichloro-5,6-dicyano-*p*-benzoquinone<sup>29</sup> as catalysts in HOAc at room temperature. Reaction of **9** with Nafion- $\text{H}^{+30}$  or  $\text{H}_2\text{SO}_4$  in HOAc at 110 °C caused desilylation. Neat HOAc, NaOAc in HOAc,<sup>31</sup> and  $\text{Al}_2\text{O}_3$  in HOAc at elevated temperatures gave moderate yields of the desired alcohol **10** (30–50%) but also caused migration of the acetate to the C-5 position; removal of this isomer proved to be impractical. However, treatment of epoxide **9** with a catalytic amount of  $\text{H}_2\text{SO}_4$ <sup>32</sup> in HOAc under carefully defined conditions provides **10** in yields of 53–66% with very little migration of the acetate. With the suitably protected triol derivative **10** in hand, we used Ganem's procedure to introduce the enolpyruvyl ether.<sup>33</sup>

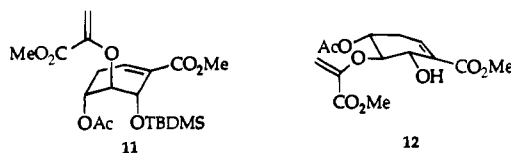
Our attempts to remove the acetate group of compound **11** under even mildly basic conditions failed (e.g., methanol with  $\text{K}_2\text{CO}_3$  or TEA), mainly giving elimination product; even treatment with tetra-*n*-butylammonium fluoride (TBAF) leads to elimination of the acetate. However, aqueous HF gives alcohol **12** in quantitative yield; hydrolysis of the esters can then be accomplished with NaOH, without elimination. Purification of the product by anion exchange chromatography, with reisolatation of the sodium salt with NaOH, gives **1** in 92% yield. Thus, racemic **1** can be synthesized in eight steps from 1-(*tert*-butyldimethylsilyloxy)-1,3-butadiene and methyl propiolate, with an overall yield of 14%.

It is puzzling that silyl ether **11** undergoes facile elimination of acetate under basic conditions while alcohol **12** undergoes practically no elimination (about 2%) when treated with a variety of bases ( $\text{K}_2\text{CO}_3$ , NaOH). An explanation for this reactivity based on the equilibrium conformations of these two compounds

Scheme 5



is supported by  $^1\text{H}$  NMR data. Silyl ether **11** favors the all-axial conformation due to severe A-1,3 strain between ring substituents in the alternative, equatorial form. However, the equatorial conformation is favored by alcohol **12** since the steric interactions are relieved with the removal of the bulky TBDMS group and since the C-6 hydroxyl and the ring carboxyl can hydrogen-bond only when the former is pseudoequatorial. In its axial position in **11**, the acetate is ideally disposed for elimination, in contrast to **12**, where it is protected by its equatorial orientation.



**Synthesis of 3.** The synthesis of the 4-amino analog **3** (Scheme 5) begins with epoxide **9**, an intermediate in the synthesis of the diol **1**. Nucleophilic opening of the epoxide with azide appeared to be the most straightforward way to introduce a nitrogen moiety at C-4. However, this particular system is very sensitive to both acidic and basic conditions. Treatment of **9** with  $\text{KN}_3$  in DMF at 90 °C led to aromatized material,  $\text{NaN}_3$  in EtOH caused elimination to the conjugated cyclohexadiene, and reaction with  $\text{NaN}_3$  and  $\text{H}_2\text{SO}_4$  in EtOH gave only the solvolysis products. The best reaction conditions proved to be  $\text{NaN}_3$  buffered with  $\text{NH}_4\text{Cl}$  in MeOH, which afford

(26) Kozłowski, M. C.; Bartlett, P. A. *J. Am. Chem. Soc.* **1991**, *113*, 5897–5898.

(27) Schlessinger, R. H.; Lopes, A. *J. Org. Chem.* **1981**, *46*, 5252–5253.

(28) Posner, G. H.; Rogers, D. Z. *J. Am. Chem. Soc.* **1977**, *99*, 8208–8214.

(29) Iranpoor, N.; Baltork, I. M. *Tetrahedron Lett.* **1990**, *31*, 735–738.

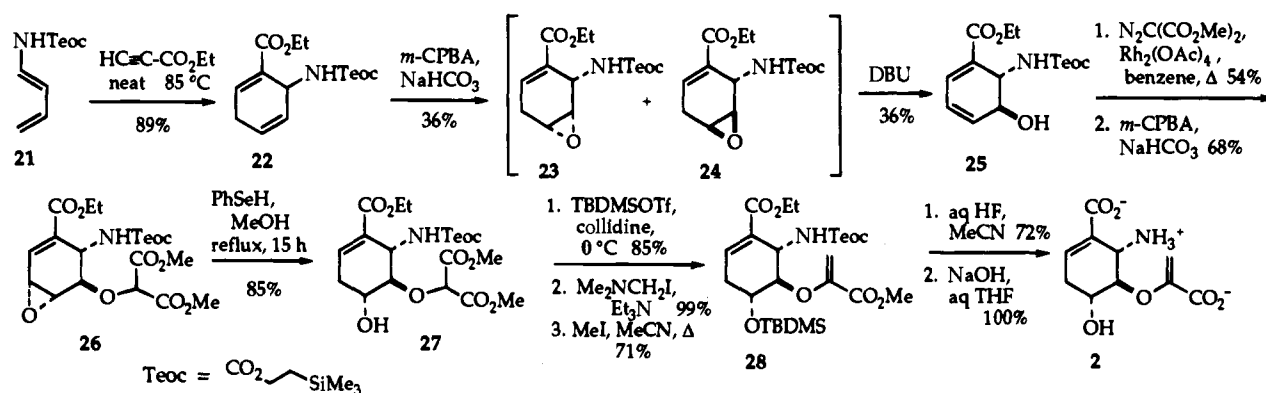
(30) Olah, G. A.; Fung, A. P.; Meidar, D. *Synthesis* **1981**, 280–282.

(31) Cope, A. C.; Grisar, J. M.; Peterson, P. E. *J. Am. Chem. Soc.* **1959**, *81*, 1640–1642.

(32) Henbest, H. B.; Smith, M.; Thomas, A. *J. Chem. Soc.* **1958**, 3293–3298.

(33) Ganem, B.; Ikota, N.; Muralidharan, V. B.; Wade, W. S.; Young, S. D.; Yukimoto, Y. *J. Am. Chem. Soc.* **1982**, *104*, 6787–6788.

Scheme 6

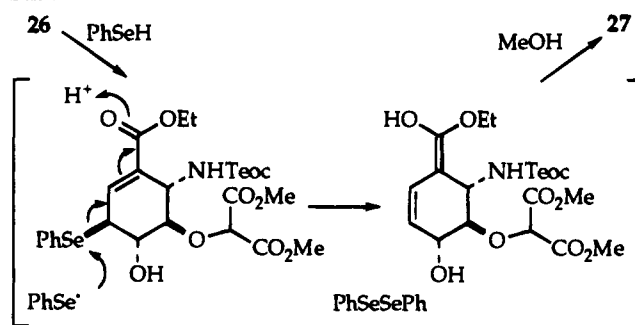


the desired azido alcohol **13** in 62% yield.<sup>34</sup> This compound forms the dimethylmalonyl ether on treatment with dimethyl diazomalonate and  $\text{Rh}_2(\text{OAc})_4$ , the first step in the sequence for introduction of the side chain.<sup>33</sup> Unfortunately, 1,3-dipolar addition of the diazo moiety to the azide and subsequent nitrogen extrusion proceed slightly more rapidly than insertion into the hydroxyl, resulting in formation of imine **18** (Scheme 5). The functionality in **18** is incompatible with the remaining steps in the reaction sequence, so an alternative, stepwise approach was adopted. Azide **13** is readily reduced with Lindlar's catalyst<sup>35</sup> to give the amino alcohol, which can be treated directly with *tert*-butyl dicarbonate<sup>36</sup> to give the protected derivative **14**. Attachment of the side chain then proceeds without complication to give the fully protected product **15**.<sup>33</sup>

A variety of protocols were explored for removal of the protecting groups, but it soon became clear that hydrolysis of the methyl esters prior to cleavage of the Boc group is obligatory; otherwise, neutralization of the amino ester leads inexorably to the lactam **19** (Scheme 5). Cleavage of the silyl ether and hydrolysis of the esters is best carried out in that order, first using tetra-*n*-butylammonium fluoride (TBAF) at 0 °C and then aqueous NaOH. More vigorous conditions for silyl ether removal lead to formation of lactone **20** (Scheme 5), which is difficult to separate from the tetra-*n*-butylammonium salts prior to hydrolysis. Diacid **17** is isolated in nearly quantitative yield from diester **16** on treatment of the saponification mixture with Dowex- $\text{H}^+$ . Removal of the Boc protecting group from **17** is easily effected with TFA, without concomitant lactam formation. Purification of the final product by anion exchange chromatography followed by treatment with aqueous NaOH provides the sodium salt of **3** in 88% yield. The synthesis of racemic **3** proceeds in an overall yield of 9% in 11 steps from 1-(*tert*-butyldimethylsilyloxy)-1,3-butadiene and methyl propiolate.

**Synthesis of 2.** The synthesis of bisubstrate analog **2** was intended to parallel that of the dihydroxy compound **1**, starting with a protected 1-aminobutadiene. The 2-(triethylsilyloxy)-carbonyl- (Teoc-) protected diene **21** is generated in 56% yield using a modified procedure.<sup>37</sup> Diels-Alder adduct **22** is formed in 89% yield by reaction of the diene with ethyl propiolate (Scheme 6), which represents a significant improvement over the reported process for the *N*-Boc derivative.<sup>16</sup> Epoxidation of cyclohexadiene **22** gives predominantly the undesired, *cis* epoxide **23**, presumably as a result of hydrogen bonding between

Scheme 7



the carbamate hydrogen and *m*-CPBA.<sup>38</sup> Various conditions and epoxidizing agents were explored in an attempt to enhance the yield of the desired *trans* isomer **24**, but to no avail. Moreover, separation of these epoxides proved to be difficult on a large scale because of the similarity in their  $R_f$  values. Finally, our efforts to open the epoxide of **24** at C-4, in analogy to the conversion of **9** to **10**, were also unsuccessful.

Our alternative strategy took advantage of the preferential elimination of *trans* epoxide **24** to the diene alcohol **25**, under conditions that lead to further elimination and aromatization of the *cis* isomer. This mixture is readily purified to provide **25** in 36% overall yield.<sup>16</sup> Although **25** aromatizes under the acidic or basic conditions normally used for attachment of several common protecting groups, the rhodium-catalyzed insertion of diazomalonate<sup>15</sup> converts it cleanly to the malonyl ether. Epoxidation of this material then affords the *trans* epoxide **26**, which represents introduction of oxygen at C-4 in the correct configuration.

Reduction of the epoxide **26** could not be accomplished, although a number of hydride reagents were explored. We therefore evaluated addition reactions involving silyl halides and organoselenium reagents, with the expectation that the halide or selenide substituent could be removed reductively. Although  $\text{TMSBr}/\text{PPh}_3$ ,  $\text{TMSCl}/\text{PPh}_3$ ,<sup>39</sup> and  $\text{PhSeSePh}/\text{NaBH}_4$ <sup>40</sup> are ineffective in this case, a modified procedure of Posner and Rogers using benzeneselenol<sup>28</sup> converts **26** directly to alcohol **27** in 85% yield. A proposed mechanism for this conversion is shown in Scheme 7. Similar reductions have been observed with sulfides, selenides, and tellurides in electronically related systems.<sup>41,42</sup>

(34) Shaw, K. J.; Luly, J. R.; Rapoport, H. *J. Org. Chem.* **1985**, *50*, 4515-4523.

(35) Corey, E. J.; Nicolaou, K. C.; Balanson, R. D.; Machida, Y. *Synthesis* **1975**, 590-591.

(36) Tarbell, D. S.; Yamamoto, Y.; Pope, B. M. *Proc. Nat. Acad. Sci. U.S.A.* **1972**, *69*, 730-732.

(37) Jessup, P. J.; Petty, C. B.; Roos, J.; Overman, L. E. *Org. Synth.* **1979**, *59*, 1-9.

(38) Mohamadi, F.; Spees, M. M. *Tetrahedron Lett.* **1989**, *30*, 1309-1310.

(39) Andrews, G. C.; Crawford, T. C.; Contillo, L. G. *Tetrahedron Lett.* **1981**, *22*, 3803-3806.

(40) Sharpless, K. B.; Lauer, R. F. *J. Am. Chem. Soc.* **1973**, *95*, 2697-2699.

(41) Miyashita, M.; Suzuki, T.; Yoshikoshi, A. *Tetrahedron Lett.* **1987**, *28*, 4293-4296.

The alcohol of **27** is silylated under standard conditions, and the malonyl ether is carried on to the enolpyruvyl ether **28** in good overall yield.<sup>15</sup> Removal of the silyl protecting groups affords the amino alcohol, and subsequent saponification and purification by anion exchange chromatography give the desired target **2** without complication. In contrast to the precursors of the isomeric amino alcohol **3**, in this system there is much less tendency for the amino ester intermediates to lactamize. The complete synthesis of racemic **2** from ethyl propiolate and diene **21** involves 11 steps and proceeds with an overall yield of 4%.

**Enzyme Assays.** Compounds **1–3** were assayed as inhibitors of IS in the forward direction using a coupled assay with isochorismatase;<sup>13</sup> the assay was performed on several occasions, with  $K_m$  values from 7.0–13.6  $\mu\text{M}$ .<sup>43</sup> AS activity was determined by a fluorimetric assay to measure anthranilate formation;<sup>44</sup> the observed values for  $K_m$  were 4.8–6.5  $\mu\text{M}$ . The PABS assays did not prove to be nearly so straightforward. Three procedures have been reported: an end-point fluorimetric assay,<sup>45</sup> a continuous lactate dehydrogenase (LDH)-coupled UV assay,<sup>21</sup> and an HPLC assay in which formation of the ADC intermediate is monitored.<sup>20</sup> The LDH-coupled UV assay reports the rate of pyruvate formation from PABS-III-catalyzed elimination of ADC. We found a very high background rate with this method (more than one-half the total rate at  $[S] = 2 \times K_m$ ), so we undertook a systematic study to determine and eliminate its causes.

The high background rate was traced to dithiothreitol (DTT) and glycerol. Although the latter could be replaced as a stabilizer by bovine serum albumin (BSA), DTT is necessary because the PABS-II component is oxidatively unstable. Attempts to replace glutamine and PABS-II with  $(\text{NH}_4)_2\text{SO}_4$  as the ammonia source were only partially successful. Although very low background rates were then observed ( $\leq 3\%$  of rate at  $[S] = 2 \times K_m$ ), the reaction progress no longer followed a simple exponential curve.

The original LDH-coupled UV assay procedure calls for 5 mM DTT in all buffers. As PABS-II is diluted into these buffers, it is reduced and DTT is oxidized; upon initiation of the assay, the oxidized DTT in turn is reduced by NADH, resulting in a signal burst. This burst can be eliminated by preincubation prior to initiating the assay with substrate; however, the large quantity of DTT present in the buffers is subject to air oxidation during the course of the assay, thereby leading to ongoing oxidation of NADH and significant background rates. Although a minimum of 10 mM DTT is required in the buffer used to dilute the PABS-II stock solutions, it can be removed from the other buffer solutions without deleterious effect.

Despite these precautions, the background rate was still significant ( $\approx 20\%$  of rate at  $[S] = 2K_m$ ), so data for the  $K_m$  and  $K_i$  determinations were only taken at substrate concentrations above  $K_m$ , which was consistently observed to be 2.0–2.75  $\mu\text{M}$ . Compounds **1** and **3** were found to be competitive inhibitors of PABS as shown by the Lineweaver–Burk plots (Figure 1 is one example); compound **2** was evaluated by Dixon analysis on the assumption that inhibition is competitive. These  $K_i$  values are given in Table 1.

Compounds **1–3** were also assayed as potential inhibitors

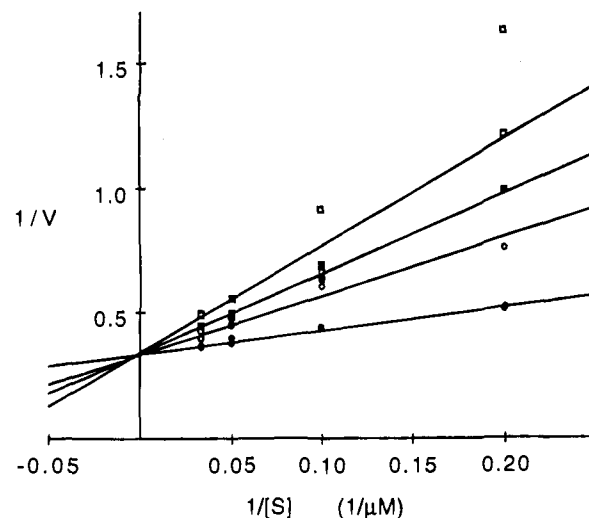


**Figure 1.** Lineweaver–Burk plot for inhibition of PABS by **1**: inhibitor concentrations = 0 (●), 100  $\mu\text{M}$  (○), 250  $\mu\text{M}$  (■), and 500  $\mu\text{M}$  (□).

**Table 1.** Summary of Observed and Normalized Inhibition Constants for IS, AS, and PABS

enzyme	ligand			
	chorismate, $K_M$ ( $\mu\text{M}$ )	<b>1</b> , $K_i$ ( $\mu\text{M}$ )	<b>2</b> , $K_i$ ( $\mu\text{M}$ )	<b>3</b> , $K_i$ ( $\mu\text{M}$ )
IS	11.5 $\pm$ 0.7	0.36 $\pm$ 0.05 <sup>a</sup>	0.053 $\pm$ 0.003	0.45 $\pm$ 0.02
AS	5.4 $\pm$ 0.3	195 $\pm$ 15 <sup>a</sup>	0.62 $\pm$ 0.04	6.3 $\pm$ 0.3
PABS	2.8 $\pm$ 0.3	124 $\pm$ 20	635 $\pm$ 102	38 $\pm$ 3
% axial ( $f_{Ax}$ )	12 <sup>b</sup>	15 <sup>c</sup>	25 <sup>c</sup>	6 <sup>c</sup>
IS norm <sup>d</sup>	1.38	0.054	0.013	0.027
AS norm <sup>d</sup>	0.65	29	0.16	0.38
PABS norm <sup>d</sup>	0.34	19	159	2.3

<sup>a</sup> Data from ref 26. <sup>b</sup> From ref 52. <sup>c</sup> Values represent the midpoints of ranges from Table 2. <sup>d</sup>  $K_i$  values normalized by  $f_{Ax}$  (Table 2); no error limits are given because of uncertainty in  $f_{Ax}$ .

of chorismate mutase/prephenate dehydrogenase (T-protein) from *E. coli*, following published procedures;<sup>46,47</sup> however, no inhibition was observed, even at high micromolar concentrations (500, 800, and 1600  $\mu\text{M}$ , respectively). The crystal structure of the monofunctional chorismate mutase from *Bacillus subtilis* complexed with a transition state analog shows that any substituent at C-6 (according to the numbering scheme for the inhibitors) would have very poor van der Waals and electrostatic interactions with a nonpolar portion of the site.<sup>48</sup> Although the active sites of these two proteins are not the same, a functional similarity of the *B. subtilis* enzyme to the other bacterial mutases has been established.<sup>49</sup> These results are also consistent with the known preference of the *E. coli* enzyme for the cross-conjugated diene system of chorismate.<sup>50,51</sup>

**Determination of Conformational Equilibria of 1–3.** Since inhibitors **1–3** were designed to mimic a transition state in which all the substituents are axial (Scheme 1), it is important to know the relative populations of the axial (Ax) and equatorial (Eq) conformations of these compounds to interpret the binding

(42) Francisco, C. G.; Freire, R.; Rodríguez, M. S.; Suarez, E. *Tetrahedron Lett.* **1991**, 32, 3413–3416.

(43) An alternative, more sensitive assay in the reverse direction, involving AS as a coupling enzyme,<sup>13</sup> is not applicable since **1–3** inhibit AS as well.

(44) Zalkin, H. In *Methods in Enzymology*; Academic Press: New York, 1985; Vol. 113, pp 287–292.

(45) Zalkin, H. In *Methods in Enzymology*; Academic Press: New York, 1985; Vol. 113, pp 293–297.

(46) Bartlett, P. A.; Johnson, C. R. *J. Am. Chem. Soc.* **1985**, 107, 7792–7793.

(47) Bartlett, P. A.; Nakagawa, Y.; Johnson, C. R.; Reich, S. H.; Luis, A. J. *Org. Chem.* **1988**, 53, 3195–3210.

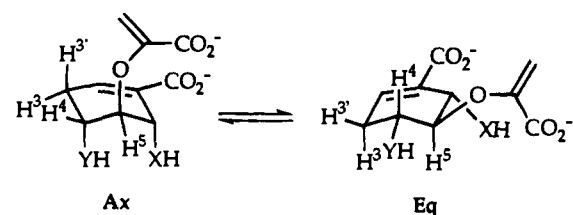
(48) Chook, Y. M.; Ke, H.; Lipscomb, W. N. *Proc. Nat. Acad. Sci. U.S.A.* **1993**, 90, 8600–8603.

(49) Gray, J. V.; Golinelli-Pimpaneau, B.; Knowles, J. R. *Biochemistry* **1990**, 29, 376–383.

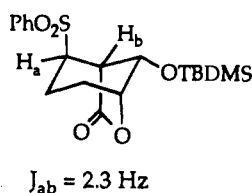
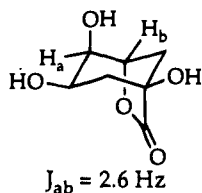
(50) Ife, R. J.; Ball, L. F.; Lowe, P.; Haslam, E. *J. Chem. Soc., Perkin Trans. 1* **1976**, 1776–1783.

(51) Christopherson, R. I.; Heyde, E.; Morrison, J. F. *Biochemistry* **1983**, 22, 1650–1656.

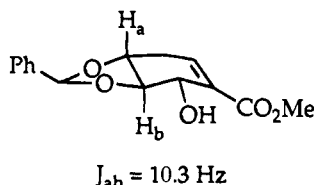
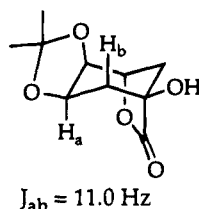
Scheme 8



Coupling constants for Ax conformation:



Coupling constants for Eq conformation:



results (Scheme 8). Eq is favored thermodynamically, but the proportion present at equilibrium is different for the three analogs as a result of hydrogen bonding and salt bridge formation. The position of equilibrium can be determined from the values of  $J_{3,4}$  and  $J_{4,5}$ , vicinal  $^1\text{H}-^1\text{H}$  coupling constants that are a direct function of the dihedral relationship between the C-H bonds.<sup>52</sup> In a molecule that undergoes conformational interconversion rapidly on the NMR time scale, the observed coupling constant is the weighted average of values from the individual conformers and therefore reflects the equilibrium composition. This relationship is expressed in eq 1, where  $J_{\text{Ax}}$

$$J_{\text{obs}} = J_{\text{Ax}}(f_{\text{Ax}}) + J_{\text{Eq}}(1 - f_{\text{Ax}}) \quad (1)$$

and  $J_{\text{Eq}}$  represent the limiting values of the coupling constant in the individual conformers and  $f_{\text{Ax}}$  is the mole fraction in the Ax conformation.  $J_{\text{Ax}}$  and  $J_{\text{Eq}}$  can be estimated from coupling constants between similar hydrogens in related compounds that are conformationally locked (Scheme 8). From these limiting values, a range of solutions can be calculated for  $f_{\text{Ax}}$  for the three inhibitors, corresponding to 10–19%, 20–28%, and 1–11% axial conformers for **1**, **2**, and **3**, respectively (Table 2). These percentages can be compared to the approximately 12% axial composition of chorismate in water, determined by Copley and Knowles.<sup>52</sup>

The temperature dependence of the coupling constants was also analyzed, as described by Bowmaker et al. (data not shown).<sup>53</sup> In addition to  $J_{3,4}$  and  $J_{4,5}$ , the geminal coupling constants  $J_{3,3'}$  were measured for the three inhibitors, over a range of temperatures in aqueous solution at assay pH. The geminal  $J_{3,3'}$  coupling constants are unaffected by temperature, as expected for a relationship that does not change with conformation, thus indicating that the intrinsic coupling con-

(52) Copley, S. D.; Knowles, J. R. *J. Am. Chem. Soc.* **1987**, *109*, 5008–5013.

(53) Bowmaker, G. A.; Calvert, D. J.; de la Mare, P. B. D.; Jones, A. J. *Org. Magn. Reson.* **1982**, *20*, 191.

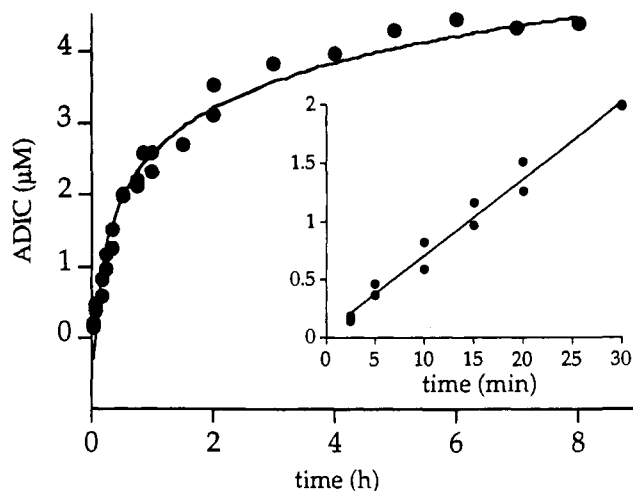


**Figure 2.** Production of ADIC by IS in the presence of 50 mM  $(\text{NH}_4)_2\text{SO}_4$ . Insert: linear portion of the curve from which the rate constant was calculated.

stants are independent of temperature. Although  $J_{3,4}$  and  $J_{4,5}$  vary in a linear fashion over the temperature ranges, they parallel each other so closely in each case that the data can not be used to reduce the uncertainty in the limiting values of  $J_{\text{Ax}}$  or  $J_{\text{Eq}}$ . The possible values for  $f_{\text{Ax}}$  given in Table 2 span a broad range, but they suggest that amino alcohol **3** has the smallest, and its isomer **2** the largest, fraction of axial conformer at equilibrium. As a basis for comparison, the midpoints of these ranges are given in Table 1 and used to normalize the inhibition constants to the percentage of axial conformer.

**HPLC Assays.** Considering all the inhibition data, we were struck by the anomalously high affinity of compound **2** toward IS. Since this enzyme does not discriminate against an amino substituent in preference to hydroxyl at C-6, we proposed that it might accept ammonia as a substrate in place of water and lead to the formation of ADIC. This premise was tested by running a discontinuous, reverse phase HPLC assay of IS in the presence of 30  $\mu\text{M}$  chorismate and 50 mM  $(\text{NH}_4)_2\text{SO}_4$  at pH 8.0. Rate determinations were possible since ADIC, isochorismate, and chorismate elute as well-separated, easily quantitated peaks.<sup>17</sup>

IS converts chorismate to both isochorismate and ADIC in the presence of ammonia. The reaction is reversible: In the absence of ammonia, IS converts ADIC quantitatively to a mixture of chorismate and isochorismate. During the course of the reaction, chorismate isomerizes to prephenate and isochorismate and ADIC undergo their respective Claisen rearrangement reactions, which complicates analysis of the HPLC data. After correction for this loss of material from the equilibrium, corresponding to 25% of the total material after 30 min, the pseudo-first-order rates of formation of both isochorismate ( $V = 2.63 \mu\text{M}/\text{min}$ ) and ADIC ( $V = 0.066 \mu\text{M}/\text{min}$ ) could be calculated (Figure 2). Thus, IS forms isochorismate 40 times faster than ADIC in the presence of 30  $\mu\text{M}$  chorismate and 50 mM  $(\text{NH}_4)_2\text{SO}_4$ .

Not unexpectedly, at 50 mM  $(\text{NH}_4)_2\text{SO}_4$ , the rate of isochorismate formation by IS is reduced by 25%. Although partial denaturation of the protein could be responsible, this inhibition may also reflect competition of the ammonia with either water or chorismate for binding sites on IS. The magnesium ion putatively responsible for coordinating the two substrates (water and chorismate) is a likely candidate for this site.

Control experiments were performed to ensure that these results were not due to contamination of the IS preparation by spurious AS. Since IS is incapable of producing anthranilate,

**Table 2.** Mole Fraction of Axial Conformer ( $f_{\text{Ax}}$ ) for **1**, **2**, and **3** as a Function of Limiting Values of  $J_{\text{Ax}}$  and  $J_{\text{Eq}}^a$ 

reference $J$ 's <sup>b</sup>		$f_{\text{Ax}}$ : <b>1</b>		$f_{\text{Ax}}$ : <b>2</b>		$f_{\text{Ax}}$ : <b>3</b>	
$J_{\text{Ax}}$	$J_{\text{Eq}}$	$J_{3,4} = 9.40$	$J_{4,5} = 9.52$	$J_{3,4} = 8.62$	$J_{4,5} = 8.70$	$J_{3,4} = 10.06$	$J_{4,5} = 10.23$
2.3	11	0.18	0.17	0.27	0.26	0.11	0.09
2.6	11	0.19	0.18	0.28	0.27	0.11	0.09
2.3	10.3	0.11	0.10	0.21	0.20	0.03	0.01
2.6	10.3	0.12	0.10	0.22	0.21	0.03	0.01

<sup>a</sup> The first two columns in the table indicate the values of  $J_{\text{Ax}}$  and  $J_{\text{Eq}}$  used in eq 1 (see Scheme 8); for each compound, the first column represents the value calculated for  $f_{\text{Ax}}$  using  $J_{3,4}$  as  $J_{\text{obs}}$  and the second column represents the value calculated from  $J_{4,5}$ . Coupling constants given for  $J_{3,4}$  and  $J_{4,5}$  for each compound are values observed at 298 K. <sup>b</sup> Note:  $J_{\text{Ax}}$  is the coupling constant for the axial conformation, in which the vicinal hydrogens are both equatorial, and *vice versa* for  $J_{\text{Eq}}$ .

AS activity was monitored by observing the rate of anthranilate formation fluorimetrically. The rate observed was negligible, corresponding to  $\leq 0.03\%$  of the rate of formation of isochorismate and  $\leq 1.3\%$  of the rate of formation of ADIC. Furthermore, a slow increase in fluorescence was also observed in the absence of ammonia, suggesting that it can be attributed to isochorismate and ADIC themselves, rather than to formation of anthranilate from contaminating AS activity.<sup>54</sup>

The HPLC data also provided a rough estimation of the equilibrium constants. The values of  $K_{\text{eq}} = 0.55$  found for the conversion of chorismate to isochorismate and  $K_{\text{eq}} = 2.67 \text{ M}^{-1}$  for conversion of chorismate and ammonia to ADIC are in good agreement with those reported by Liu et al.<sup>13</sup> and by Morollo and Bauerle,<sup>17</sup> respectively. Together, these values imply that  $K_{\text{eq}}$  for the conversion of isochorismate and ammonia to ADIC is  $4.80 \text{ M}^{-1}$  ( $\Delta G = -0.97 \text{ kcal/mol}$ ).<sup>55</sup>

## Discussion

**Inhibitor Selectivity.** The inhibition constants for the racemic inhibitors **1**, **2**, and **3** against IS, AS, and PABS are summarized in Table 1. These values are not corrected for the presence of the enantiomer; if only one is responsible for binding, the actual values could be smaller by a factor of 2. Table 1 also includes the  $K_i$  values after normalization for the percentage of each inhibitor that exists in the axial conformation. The inhibitors bind to IS with significantly higher affinity than the substrate, as suggested by its  $K_m$  value; for AS, the difference is not as great, but the amino alcohols are bound 2–4-fold as tightly (normalized values). For PABS, all inhibitors are significantly weaker than substrate in their affinity.

Although compound **2** was designed as a specific inhibitor of AS, it proved to be the most potent inhibitor of IS as well. To some extent, the higher affinity observed for **2** is due to the greater proportion of this analog that exists in the axial conformation. Selective binding by IS and AS of the axial forms of these inhibitors might provide a partial explanation for this phenomenon, since the inhibitor with the highest observed affinity, amino alcohol **2**, has the highest proportion of this conformer. The normalized data indicate that *both* of the amino alcohols **2** and **3** are more potent inhibitors of IS, as well as of AS, than diol **1**.

The relatively poor binding of diol **1** to AS is understandable since it must select against hydroxyl groups; otherwise AS would produce isochorismate from reaction with water, instead

of ADIC. There is no complementary preference in the case of IS, since free ammonia is not available *in vivo* and there has been no evolutionary pressure for IS to select against ammonia as a substrate. This interpretation is confirmed by the ability of IS to produce ADIC as well as isochorismate. That IS and AS can generate the same product is additional evidence that they are functionally related.

**IS and AS Mechanisms.** A variety of mechanisms have been considered for the reactions catalyzed by IS and AS (Scheme 9).<sup>3</sup> Path A, direct substitution of the C-4 hydroxyl with the C-6 substituent, can itself embrace a range of possibilities. The process could be concerted, with simultaneous bond cleavage and formation, or it could be stepwise, with the transition state carrying either cationic character in the ring system (bond-cleavage first) or anionic character (bond-formation first, with delocalization of the charge into the carboxyl group). Any of this spectrum of possibilities could be mediated by coordination of the reactants with magnesium as depicted. The involvement of the magnesium cation is suggested by observations that it is required for activity and that it is coordinated to chorismate at the AS active site.<sup>23</sup>

Although high affinity alone is no proof that an inhibitor is a transition state or multisubstrate analog, it is unlikely that we would observe this pattern of inhibition for compounds **1–3** with IS and AS if their mechanisms differ radically from that depicted in Scheme 9, path A, or if the inhibitors bind in some fortuitous or irrelevant mode. This argument is strengthened by the fact that these analogs are significantly worse as inhibitors of PABS, an enzyme whose mechanism must differ substantially from those of IS and AS. The relative affinities of the inhibitors provide further insights. The similar affinities of the isomeric amino alcohols **2** and **3** toward either AS or IS imply that they operate through symmetrical or quasi-symmetrical transition states. Two explanations for the higher affinities of the amino alcohols in comparison to the diol **1** can be invoked: On the one hand, the zwitterionic nature of the amino alcohols at neutral pH may imitate the charges in the transition state better, if it proceeds through a cationic mechanism. Alternatively, the amino group may better coordinate the magnesium ion or another acid/Lewis acid functional group in the active site.<sup>57</sup>

The most likely alternatives to path A involve transient nucleophilic attack at the C-2 carbon, either by an enzyme-bound "X-group", the enolpyruvyl side chain carboxylate, or water (paths B1–B3). The fact that the epoxy analog **29** is not a potent or irreversible inhibitor of AS suggests that nucleophilic attack from the  $\beta$ -face, either by X-group or side chain, is not involved.<sup>56</sup> The product from attack of water from

(54) Having observed ADIC formation by IS, we asked whether AS might display analogous behavior and convert chorismate to isochorismate. Although we attempted to observe this reaction, our supplies of wild type AS and AS-I were contaminated with IS activity, which precluded use of these preparations to test the hypothesis. The absence of fluorimetrically observable anthranilate formation in the presence of  $100 \mu\text{M}$  L-tryptophan ( $K_i = 1\text{--}5 \mu\text{M}$ )<sup>17</sup> indicated that the AS activity is completely inhibited. However, isochorismate formation was still observed under these conditions, which implied that the AS was contaminated with residual IS activity.

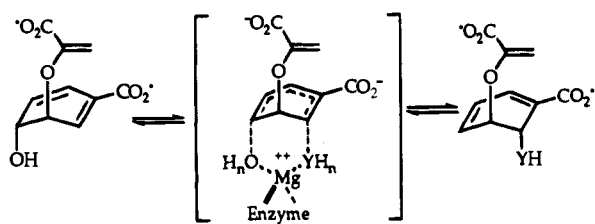
(55) The equilibrium constants were calculated at  $30 \mu\text{M}$  chorismate and  $50 \text{ mM}$   $(\text{NH}_4)_2\text{SO}_4$  and include the concentration of ammonium ions.

(56) Walsh, C. T.; Erion, M. D.; Walts, A. E.; Delany, J. J.; Berchtold, G. A. *Biochemistry* **1987**, *26*, 4734–4745.

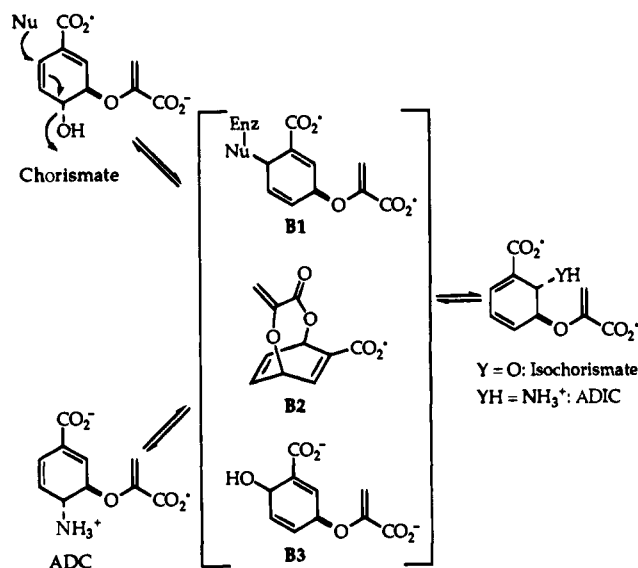
(57) A single amine ligand for magnesium is bound favorably with respect to water: Goodenough, R. D.; Stenger, V. A. In *Comprehensive Inorganic Chemistry*; Bailar, J. C., Jr., Emeléus, H. J., Nyholm, R., Trotman-Dickenson, A. F., Eds.; Pergamon Press: Oxford, U.K., 1973; Vol. 1, p 664.

## Scheme 9

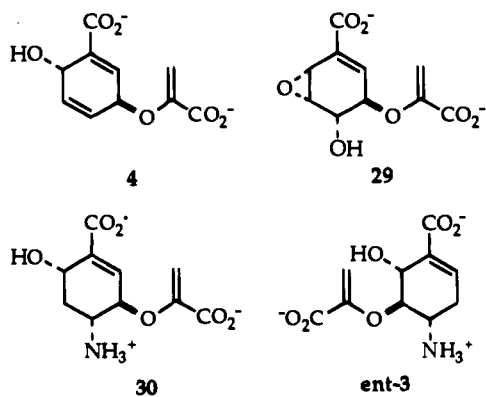
## Mechanism A



## Mechanism B

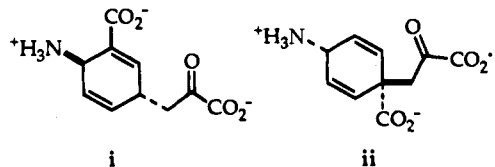


the  $\alpha$ -face, compound **4**, was synthesized by Mattia and Ganem to see if this species is involved in the PABS mechanism, and in the IS and AS reactions as well.<sup>25</sup> Unfortunately, Claisen rearrangement of this material proved to be so rapid under the assay conditions that it could not be evaluated as an alternative substrate for these enzymes.<sup>58</sup>



**PABS Mechanism.** The modest affinity of the three inhibitors for PABS is consistent with the likelihood that nucleophilic attack at C-6 does not occur in the course of the substitution

(58) While Ganem et al. have shown that the amino analogs **i** and **ii** (which bear some resemblance to **4**) inhibit AS<sup>15</sup> and PABS,<sup>19</sup> respectively, it is difficult to gauge the significance of these results without the inhibition constants, which were not reported.



process. Among the inhibitors, the higher affinity of the 4-amino isomer **3** reflects its greater similarity to the initial substitution product, ADC. In contrast to IS and AS, sequential path B mechanisms, rather than direct substitution, are implicated in the PABS-catalyzed reaction. Of the two likely double-displacement processes that can be envisaged, sequential 1,5-substitutions via isochorismate have been ruled out.<sup>19,24</sup> The poor binding affinity of compounds **1–3** for PABS, and in particular the contrast with their affinity for IS and AS, is entirely consistent with this interpretation. The isomeric derivative **30** would be a useful probe for the alternative mechanism, which involves sequential 1,3-substitutions via **4**. The enantiomer of **3** mimics **30** in some respects but could only do so effectively if the enolpyruvyl side chain were bound on top of the cyclohexenyl ring, an unlikely orientation because of steric crowding and risk of Claisen rearrangement in the normal substrate.

## Conclusion

The success of these inhibitors not only provided supporting evidence for the proposed transition state on which their design was based, mechanism A of Scheme 9, but also revealed a number of similarities and differences between the three evolutionarily related enzyme targets. Further insight may be gained from structural studies with these compounds and when the isomeric analogs are available that are potentially more appropriate as transition state analogs of PABS (mechanism B of Scheme 9).

Experimental Section<sup>59</sup>

**Sodium (4*R*\*,5*S*\*,6*S*\*)-5-[(1-Carboxyethenyl)oxy]-4,6-dihydroxycyclohex-1-enecarboxylate (1).** Full experimental details for the synthesis of **1** are found in the supplementary material of its first report.<sup>26</sup>

**(4*S*\*,5*R*\*,6*R*\*)-4-Hydroxy-5-[(1-carboxyethenyl)oxy]-6-aminocyclohex-1-enecarboxylic Acid (2).** Enol ether **28** (see below) (0.407 g, 0.748 mmol) was dissolved in acetonitrile (50 mL) in a Nalgene container. Aqueous HF (3.5 mL, 50% solution) was added, and the reaction mixture was allowed to stand at room temperature for 4 h. The reaction was quenched by slowly adding the solution to 100 mL of saturated aqueous NaHCO<sub>3</sub>. The aqueous layer was extracted with CHCl<sub>3</sub> (3 × 75 mL), the organic extracts were combined and dried over MgSO<sub>4</sub>, and the solvent was removed. The crude material was purified by flash chromatography using 2.5% MeOH/CH<sub>2</sub>Cl<sub>2</sub> to give the amino alcohol (0.153 g, 72%): <sup>1</sup>H NMR (400 MHz, CDCl<sub>3</sub>)  $\delta$  1.08 (dd, 1, *J* = 3.9, 4.6), 5.52 (d, 1, *J* = 2.7), 4.95 (d, 1, *J* = 2.7), 4.18–4.26 (m, 4), 4.04 (br s, 1), 3.77 (s, 3), 3.05 (br s, 3), 2.66 (dm, 1, *J* = 19.8), 2.48 (app dt, 1, *J* = 3.8, 19.6), 1.32 (t, 3, *J* = 7.1); <sup>13</sup>C NMR (100 MHz, CDCl<sub>3</sub>)  $\delta$  166.3, 163.6, 149.9, 138.6, 129.4, 98.4, 77.5, 65.0, 60.7, 52.4, 47.7, 31.4, 14.2; HRMS-FAB (MH<sup>+</sup>) calcd for C<sub>13</sub>H<sub>20</sub>NO<sub>6</sub> 286.1291, found 286.1284. Anal. Calcd for C<sub>13</sub>H<sub>19</sub>NO<sub>6</sub>: C, 54.73; H, 6.71; N, 4.91. Found: C, 54.55; H, 6.64; N, 4.95.

The amino alcohol (26.1 mg, 91.5  $\mu$ mol) was dissolved in D<sub>2</sub>O (3.5 mL) in a 5-mm NMR tube. To the solution was added 0.125 g of 30% NaOD/D<sub>2</sub>O (w/v), and the hydrolysis reaction was monitored by <sup>1</sup>H NMR spectroscopy. After 5 h, the reaction was diluted with H<sub>2</sub>O (2 mL) and 800  $\mu$ L of 1 N HCl was added to give a pH of 8–9. The

(59) **General Procedures.** Reagents and solvents were obtained from commercial suppliers and were used as received, unless otherwise noted. All moisture- or air-sensitive reactions were conducted under nitrogen in dried solvents. Column chromatography was performed by the method of Still, Kahn, and Mitra using 60-mesh silica gel from Merck.<sup>60</sup> All <sup>13</sup>C NMR spectra were proton decoupled. Spectral data are reported (multiplicity, number of hydrogens, coupling constants in hertz) relative to tetramethylsilane for <sup>1</sup>H NMR and CDCl<sub>3</sub> (77.0 ppm) or MeOH (49.0 ppm) for <sup>13</sup>C NMR spectra unless otherwise noted. Combustion analyses were performed by the Microanalytical Laboratory, College of Chemistry, University of California, Berkeley.

(60) Still, W. C.; Kahn, M.; Mitra, A. J. *J. Org. Chem.* **1978**, *43*, 2923–2925.



mixture was lyophilized, and the crude material was purified by ion exchange chromatography on DEAE Sephadex A25 (1 × 11 cm column, HCO<sub>3</sub><sup>-</sup> form), eluted with a gradient of 0.0–0.2 M TBK buffer, pH 8.3. Fractions absorbing at 240 nm were pooled and lyophilized, and the residue was dissolved in a minimum amount of water and passed through a column of Dowex 50 X2-400 (1 × 10 cm, Na<sup>+</sup> form). The column was eluted with water, and fractions that absorbed at 240 nm were pooled and lyophilized to give the disodium salt of **2**: <sup>1</sup>H NMR (400 MHz, D<sub>2</sub>O) δ 6.74 (m, 1), 5.18 (d, 1, *J* = 2.7), 4.80 (d, 1, *J* = 2.6), 4.17 (m, 1), 4.09 (dm, 1, *J* = 7.5), 3.98 (m, 1), 2.60 (dt, 1, *J* = 5.4, 19.0), 2.26 (ddt, 1, *J* = 8.6, 19.1); <sup>13</sup>C NMR (100 MHz, D<sub>2</sub>O) δ 172.0, 170.7, 155.5, 138.2, 128.2, 97.1, 79.7, 67.3, 52.3, 31.7.

**Sodium (4*R*\*,5*S*\*,6*S*\*)-4-Amino-5-[(1-carboxyethenyl)oxy]-6-hydroxycyclohex-1-enecarboxylate (3).** Cold, dry TFA (0 °C) was added via cannula to compound **17** (see below) (0.208 g, 0.61 mmol), which was also cooled to 0 °C. After 15 min, the reaction mixture was cooled further to –78 °C and the TFA was removed *in vacuo*. The resulting oil was dissolved in H<sub>2</sub>O and lyophilized to give the TFA salt as a pale yellow powder: <sup>1</sup>H NMR (300 MHz, D<sub>2</sub>O) δ 6.77 (s, 1), 5.51 (s, 1), 5.12 (s, 1), 4.56 (s, 1), 4.30 (s, 1), 3.58 (s, 1), 2.68 (m, 1), 2.41 (m, 1); <sup>13</sup>C NMR (100 MHz, D<sub>2</sub>O) δ 169.6, 167.2, 164.3 (TFA), 164.0 (TFA), 163.6 (TFA), 163.3 (TFA), 150.6, 138.4, 132.0, 118.8 (TFA), 115.9 (TFA), 113.0 (TFA), 103.2, 79.3, 68.5, 48.2, 28.4; MS (FAB) *m/z* calcd for MH<sup>+</sup> C<sub>10</sub>H<sub>14</sub>NO<sub>6</sub> 244.082 112, found 244.082 870, 284 (MK<sup>+</sup>), 266 (MNa<sup>+</sup>), 244 (MH<sup>+</sup>), 223, 207.

The TFA salt was neutralized to pH = 7 with 0.2 M triethylammonium bicarbonate (TBK, pH = 8.2) and applied to a 3 × 7-cm column of DEAE Sephadex A-25 (HCO<sub>3</sub><sup>-</sup> form). The column was eluted with a gradient of H<sub>2</sub>O to 0.1 M TBK, pH = 8.2, and the eluent was monitored spectrophotometrically at 254 nm. Lyophilization of the appropriate fractions afforded the triethylammonium salt as a white powder: <sup>1</sup>H NMR (400 MHz, D<sub>2</sub>O) δ 6.24 (s, 1), 5.15 (s, 1), 4.84 (s, 1), 4.49 (s, 1), 4.11 (dd, 1, *J* = 7.2, 9.1), 3.47 (dd, 1, *J* = 9.1, 14.6), 2.97 (q, 6, *J* = 7.0), 2.57 (m, 1), 2.29 (dd, 1, *J* = 9.5, 17.7), 1.05 (t, 9, *J* = 7.0); <sup>13</sup>C NMR (100 MHz, D<sub>2</sub>O) δ 174.5, 171.4, 156.4, 137.5, 130.7, 98.6, 81.5, 71.3, 49.8, 47.6, 29.1, 9.3; MS (FAB) *m/z* 289 (MNa<sub>2</sub><sup>+</sup>), 266 (MNa<sup>+</sup>), 244 (MH<sup>+</sup>), 215, 207.

The triethylammonium salt (0.165 g, 0.48 mmol) was dissolved in H<sub>2</sub>O (100 mL), and 1.0 equiv of aqueous NaOH (0.986 N, 0.487 mL, 0.48 mmol) was added. Removal of the triethylamine was accomplished by lyophilizing the resulting mixture 3 times to give sodium salt **3** in 90% calculated purity based on %C as determined by combustion analysis (for C<sub>10</sub>H<sub>12</sub>NO<sub>6</sub>Na, C: anal. calcd 45.29%, found 40.80%). Thus, sodium salt **3** (0.141 g, 90% pure, 79% yield) was obtained as a white hygroscopic powder: mp 130–131 °C; <sup>1</sup>H NMR (400 MHz, D<sub>2</sub>O) δ 6.26 (s, 1), 5.17 (s, 1), 4.83 (s, 1), 4.52 (d, 1, *J* = 4.7), 4.12 (dd, 1, *J* = 7.3, 9.3), 3.42 (ddd, 1, *J* = 5.4, 9.2, 9.2), 2.56 (ddd, 1, *J* = 4.9, 4.9, 18.2), 2.27 (dd, 1, *J* = 9.6, 17.8); <sup>13</sup>C NMR (100 MHz, DMSO-*d*<sub>6</sub>) δ 174.9, 171.5, 156.2, 137.6, 130.7, 98.3, 81.6, 71.5, 49.8, 29.2; IR (KBr) 3421, 2363, 1560, 1400, 1221, 1062 cm<sup>-1</sup>; MS (FAB) *m/z* 332 (MNa<sub>2</sub><sup>+</sup>), 310 (MNa<sub>3</sub><sup>+</sup>), 288 (MNa<sub>2</sub><sup>+</sup>), 266 (MNa<sup>+</sup>), 244 (MH<sup>+</sup>), 237, 200.

**Methyl (4*R*\*,5*S*\*,6*S*\*)-4-Azido-6-(*tert*-butyldimethylsiloxy)-5-hydroxycyclohex-1-enecarboxylate (13).** A suspension of epoxide **9** (1.00 g, 3.54 mmol), NaN<sub>3</sub> (1.15 g, 17.7 mmol), and NH<sub>4</sub>Cl (1.14 g, 21.3 mmol) in MeOH (30 mL) was heated to reflux. After 12 h, the reaction mixture was cooled and diluted with saturated NaHCO<sub>3</sub> (200 mL) and H<sub>2</sub>O (50 mL). The resulting solution was extracted with CH<sub>2</sub>-Cl<sub>2</sub> (4 × 250 mL), and the combined organic layers were dried with MgSO<sub>4</sub> and concentrated to an oil. Purification of the crude product by flash chromatography using a gradient of 10–20% EtOAc/hexanes afforded compound **13** (0.718 g, 62%) as white crystals: mp 59.5–60.5 °C; <sup>1</sup>H NMR (400 MHz, CDCl<sub>3</sub>) δ 6.61 (ddd, 1, *J* = 0.9, 2.4, 5.9), 4.58 (dddd, 1, *J* = 1.4, 1.4, 2.8, 6.2), 3.73 (s, 3), 3.67 (ddd, 1, *J* = 3.8, 6.2, 10.0), 3.53 (ddd, 1, *J* = 5.4, 9.9, 9.9), 2.60 (dddd, 1, *J* = 1.0, 5.7, 5.7, 18.3), 2.42 (d, 1, *J* = 3.6), 2.28 (dddd, 1, *J* = 2.7, 2.7, 9.8, 18.4), 0.86 (s, 9), 0.19 (s, 3), 0.12 (s, 3); <sup>13</sup>C NMR (100 MHz, CDCl<sub>3</sub>) δ 166.6, 134.3, 133.6, 72.4, 60.5, 51.8, 51.7, 29.6, 25.9, 18.3, –4.2, –5.0; IR (film) 3470, 2930, 2850, 2100, 1720, 1250, 1100 cm<sup>-1</sup>; MS (FAB) *m/z* 328, 312, 270, 185, 153, 136, 108. Anal. Calcd for C<sub>14</sub>H<sub>25</sub>N<sub>3</sub>O<sub>4</sub>Si: C, 51.35; H, 7.70; N, 12.83. Found: C, 51.46; H, 7.78; N, 13.02.

**Methyl (4*R*\*,5*S*\*,6*S*\*)-6-(*tert*-Butyldimethylsiloxy)-4-(*tert*-butyloxycarbonyl)amino]-5-hydroxycyclohex-1-enecarboxylate (14).** A suspension of azide **13** (0.353 g, 1.10 mmol) and Lindlar's catalyst (0.106 g, 30 wt %) in EtOH (50 mL) was stirred vigorously under H<sub>2</sub> at atmospheric pressure. After 3 h, the reaction mixture was filtered through Celite and the solvent was evaporated to give the amine (0.336 g, 100%) as pale yellow crystals which were used without further purification: <sup>1</sup>H NMR (400 MHz, CDCl<sub>3</sub>) δ 6.6 (s, 1), 5.45 (d, 1, *J* = 4.5), 3.72 (s, 3), 3.51 (dd, 1, *J* = 6.0, 8.8), 2.88 (m, 1), 2.50 (ddd, 1, *J* = 5.1, 5.1, 18.4), 2.30 (s, 3), 2.12 (dd, 1, *J* = 8.4, 18.3), 0.86 (s, 9), 0.19 (s, 3), 0.12 (s, 3); <sup>13</sup>C NMR (100 MHz, CDCl<sub>3</sub>) δ 167.1, 135.7, 133.6, 77.7, 72.3, 51.6, 50.4, 33.5, 25.9, 18.2, –4.2, –5.0.

A solution of Boc<sub>2</sub>O (0.267 g, 1.20 mmol) in THF (10 mL) was added dropwise to a solution of the amine (0.336 g, 1.10 mmol) and Et<sub>3</sub>N (0.17 mL, 1.20 mmol) in THF (40 mL) over 10 min. After 25 h, MeOH (10 mL) was added and the reaction mixture was concentrated to a small volume (~10 mL). The concentrate was diluted with CH<sub>2</sub>-Cl<sub>2</sub> (250 mL), washed with saturated NH<sub>4</sub>Cl (2 × 100 mL) and saturated NaHCO<sub>3</sub> (2 × 100 mL), dried with MgSO<sub>4</sub>, and concentrated to an oil. Purification of the crude product by flash chromatography using 30% EtOAc/hexanes afforded compound **14** (0.332 g, 74%) as white crystals: mp 147–148 °C; <sup>1</sup>H NMR (400 MHz, CDCl<sub>3</sub>) δ 7.01 (d, 1, *J* = 2.2), 6.28 (d, 1, *J* = 9.0), 4.57 (d, 1, *J* = 1.0), 4.10 (t, 1, *J* = 4.1), 3.99 (m, 1), 3.75 (s, 3), 3.67 (d, 1, *J* = 3.2), 2.67 (d, 1, *J* = 19.7), 2.35 (ddd, 1, *J* = 1.1, 5.0, 19.8), 1.39 (s, 9), 0.88 (s, 9), 0.21 (s, 3), 0.11 (s, 3); <sup>13</sup>C NMR (100 MHz, CDCl<sub>3</sub>) δ 166.9, 155.4, 139.1, 129.6, 79.3, 69.5, 67.3, 51.5, 46.6, 28.7, 28.3, 25.7, 17.9, –5.0, –5.0; IR (KBr) 3520, 3480, 2940, 2850, 1715, 1700, 1515, 1245, 1160, 1040, 860 cm<sup>-1</sup>. Anal. Calcd for C<sub>19</sub>H<sub>35</sub>NO<sub>6</sub>Si: C, 56.83; H, 8.78; N, 3.49. Found: C, 57.20; H, 8.72; N, 3.74.

**Methyl (4*R*\*,5*S*\*,6*S*\*)-6-(*tert*-Butyldimethylsiloxy)-4-(*tert*-butyloxycarbonyl)amino]-5-[[1-(methoxycarbonyl)ethenyl]oxy]cyclohex-1-enecarboxylate (15).** Alcohol **14** (0.322 g, 0.80 mmol) and dimethyl diazomalonalate (0.317 g, 2.00 mmol) were dissolved in benzene (27 mL). Rh<sub>2</sub>(OAc)<sub>4</sub> (0.004 g, 0.01 mmol) was added, and the solution was heated to reflux. After 2 h, the reaction mixture was frozen and the benzene was removed *in vacuo*. Purification of the crude product by flash chromatography using 20% EtOAc/hexanes afforded the malonyl ether (0.302 g, 71%) as a clear oil: <sup>1</sup>H NMR (400 MHz, CDCl<sub>3</sub>) δ 7.04 (dd, 1, *J* = 2.1, 5.1), 6.20 (d, 1, *J* = 9.0), 4.73 (s, 1), 4.67 (s, 1), 4.18 (ddd, 1, *J* = 4.4, 4.4, 8.9), 3.82 (s, 3), 3.79 (s, 3), 3.78 (m, 1), 3.75 (s, 3), 2.63 (dddd, 1, *J* = 2.4, 2.4, 4.9, 19.8), 2.39 (dd, 1, *J* = 5.2, 19.8), 1.40 (s, 9), 0.88 (s, 9), 0.21 (s, 3), 0.14 (s, 3); <sup>13</sup>C NMR (100 MHz, CDCl<sub>3</sub>) δ 166.8, 166.3, 166.0, 155.0, 139.5, 129.0, 79.1, 77.7, 77.5, 65.4, 52.9, 52.8, 51.5, 43.3, 28.8, 28.2, 25.6, 17.8, –5.1, –5.2; IR (film) 3410, 2960, 2860, 1770, 1750, 1720, 1710, 1510 cm<sup>-1</sup>. Anal. Calcd for C<sub>24</sub>H<sub>41</sub>NO<sub>10</sub>Si: C, 54.22; H, 7.77; N, 2.63; Found: C, 54.49; H, 7.78; N, 2.80.

*N,N*-Dimethylmethyleammonium iodide (0.111 g, 0.60 mmol) was added to a solution of the malonyl ether (0.266 g, 0.50 mmol) in CH<sub>2</sub>-Cl<sub>2</sub> (10 mL), and the mixture was stirred for 5 min. Et<sub>3</sub>N (91 μL, 0.65 mmol) was added, and the solution rapidly became colorless. After 13.5 h, the reaction mixture was diluted with CH<sub>2</sub>Cl<sub>2</sub> (100 mL) and washed with H<sub>2</sub>O (50 mL), 10% Na<sub>2</sub>CO<sub>3</sub> (50 mL), and H<sub>2</sub>O (50 mL). The organic layer was dried with MgSO<sub>4</sub>, and the solvent was removed to give the Mannich base (0.294 g, 100%) as a clear oil which was used without further purification: <sup>1</sup>H NMR (400 MHz, CDCl<sub>3</sub>) δ 7.02 (d, 1, *J* = 2.7), 6.25 (d, 1, *J* = 9.1), 4.97 (s, 1), 4.16 (s, 1), 3.96 (m, 1), 3.84 (s, 3), 3.81 (s, 3), 3.74 (s, 3), 2.94 (d, 1, *J* = 13.9), 2.76 (d, 1, *J* = 14.0), 2.60 (d, 1, *J* = 19.7), 2.35 (dd, 1, *J* = 5.1, 20.0), 2.19 (s, 6), 1.38 (s, 9), 0.87 (s, 9), 0.23 (s, 3), 0.20 (s, 3); <sup>13</sup>C NMR (100 MHz, CDCl<sub>3</sub>) δ 168.4, 167.7, 165.5, 154.6, 139.1, 129.6, 86.5, 78.4, 73.6, 66.1, 63.4, 52.5, 52.1, 51.1, 47.1, 44.4, 29.0, 28.0, 25.5, 17.7, –4.9, –5.7; IR (film) 3400, 2950, 2850, 1765, 1740, 1715, 1500, 1245, 1050, 1030 cm<sup>-1</sup>; MS (FAB) *m/z* calcd for MH<sup>+</sup> C<sub>27</sub>H<sub>49</sub>N<sub>2</sub>O<sub>10</sub>Si 589.316 650, found 589.316 650, 589, 533, 344, 328, 288.

A solution of the Mannich base (0.293 g, 0.50 mmol) and MeI (0.31 mL, 4.98 mmol) in acetonitrile (25 mL) was heated to 90 °C. After 14 h, the reaction mixture was cooled, diluted with cold Et<sub>2</sub>O (50 mL), filtered through a short silica plug, and concentrated. Purification of the crude product by flash chromatography using 20% EtOAc/hexanes afforded compound **15** (0.190 g, 78%) as a clear oil: <sup>1</sup>H NMR (400

MHz, CDCl<sub>3</sub>)  $\delta$  7.06 (dd, 1,  $J$  = 2.1, 4.9), 6.13 (d, 1,  $J$  = 9.1), 5.57 (d, 1,  $J$  = 2.7), 4.90 (d, 1,  $J$  = 2.7), 4.69 (s, 1), 4.27 (s, 2), 3.76 (s, 3), 3.76 (s, 3), 2.64 (d, 1,  $J$  = 19.8), 2.42 (dd, 1,  $J$  = 5.3, 19.8), 1.41 (s, 9), 0.90 (s, 9), 0.23 (s, 3), 0.13 (s, 3); <sup>13</sup>C NMR (100 MHz, CDCl<sub>3</sub>)  $\delta$  166.2, 163.0, 154.8, 149.0, 139.1, 129.1, 98.4, 79.0, 74.7, 64.2, 52.1, 51.4, 42.8, 28.6, 28.1, 25.5, 17.8, -5.1, -5.2; IR (film) 3405, 2940, 2840, 1740, 1720, 1705, 1620 cm<sup>-1</sup>. Anal. Calcd for C<sub>23</sub>H<sub>39</sub>NO<sub>8</sub>Si: C, 56.88; H, 8.09; N, 2.88; Found: C, 56.57; H, 8.27; N, 3.04.

**Methyl (4R\*,5S\*,6S\*)-4-[(*tert*-Butyloxycarbonyl)amino]-6-hydroxy-5-[[1-(methoxycarbonyl)ethoxy]oxy]cyclohex-1-enecarboxylate (16).** TBAF (1.0 M solution in THF, 0.98 mL, 0.98 mmol) was added to a 0 °C solution of compound **15** (0.318 g, 0.65 mmol) in THF (16 mL). After 5 min, the reaction mixture was quenched with 0.5 N HCl (10 mL) at 0 °C. This solution was diluted with more 0.5 N HCl (80 mL) and extracted with EtOAc (4 × 80 mL). The combined organic extracts were dried with MgSO<sub>4</sub> and concentrated to an oil. Purification of the crude product by flash chromatography using a gradient of 20–40% EtOAc/hexanes afforded compound **16** (0.178 g, 73%) as an intractable foam: <sup>1</sup>H NMR (400 MHz, CDCl<sub>3</sub>)  $\delta$  7.06 (dd, 1,  $J$  = 2.7, 4.9), 5.79 (d, 1,  $J$  = 6.2), 5.56 (d, 1,  $J$  = 2.8), 5.00 (d, 1,  $J$  = 2.7), 4.59 (s, 1), 4.39 (dd, 1,  $J$  = 2.5, 4.6), 4.17 (s, 1), 3.79 (s, 3), 3.77 (s, 3), 3.49 (s, 1), 2.69 (ddd, 1,  $J$  = 2.0, 2.5, 19.6), 2.47 (ddd, 1,  $J$  = 3.0, 4.7, 19.6), 1.43 (s, 9); <sup>13</sup>C NMR (100 MHz, CDCl<sub>3</sub>)  $\delta$  167.0, 163.4, 155.3, 149.2, 139.6, 129.0, 98.5, 79.5, 75.3, 65.0, 52.4, 52.0, 44.3, 28.8, 28.3; IR (CH<sub>2</sub>Cl<sub>2</sub>) 3594, 3418, 2979, 2954, 2360, 1706, 1621, 1507, 1270, 1260, 1169 cm<sup>-1</sup>; MS (FAB)  $m/z$  calcd for MH<sup>+</sup> C<sub>17</sub>H<sub>26</sub>NO<sub>8</sub> 372.165 842, found 372.165 320, 394 (MNa<sup>+</sup>), 372 (MH<sup>+</sup>), 339, 316, 298, 272, 205, 196.

**(4R\*,5S\*,6S\*)-4-[(*tert*-Butyloxycarbonyl)amino]-5-[(1-carboxyethenyl)oxy]-6-hydroxycyclohex-1-enecarboxylic Acid (17).** Aqueous NaOH (1.0 N, 1.87 mL, 1.87 mmol) was added dropwise to a solution of compound **16** (0.232 g, 0.62 mmol) in THF (10 mL) and H<sub>2</sub>O (8 mL) at 0 °C. After 1.5 h, the reaction mixture was neutralized with Dowex 50-X (H<sup>+</sup>) and filtered, and the solution was lyophilized to afford compound **17** (0.208 g, 97%) as a flocculent white powder which was used without further purification: mp 115–118 °C; <sup>1</sup>H NMR (400 MHz, CD<sub>3</sub>OD)  $\delta$  6.97 (dd, 1,  $J$  = 3.7, 3.7), 5.51 (d, 1,  $J$  = 2.3), 4.60 (d, 1,  $J$  = 3.2), 4.34 (dd, 1,  $J$  = 3.9, 6.0), 3.99 (dd, 1,  $J$  = 5.1, 10.3), 2.61 (ddd, 1,  $J$  = 4.0, 4.0, 19.4), 2.39 (ddd, 1,  $J$  = 3.9, 3.9, 19.4), 1.41 (s, 9); <sup>13</sup>C NMR (100 MHz, CD<sub>3</sub>OD)  $\delta$  169.3, 166.2, 157.4, 151.5, 139.5, 131.9, 98.2, 80.5, 79.0, 66.7, 46.9, 30.2, 28.7; IR (KBr) 3396, 2980, 1700, 1522, 1395, 1368, 1253, 1168 cm<sup>-1</sup>; MS (FAB)  $m/z$  calcd for MH<sup>+</sup> C<sub>15</sub>H<sub>22</sub>NO<sub>8</sub> 344.134 542, found 344.134 690, 382 (MK<sup>+</sup>), 366 (MNa<sup>+</sup>), 344 (MH<sup>+</sup>), 302, 288, 244.

**1-[[[2-(Trimethylsilyl)ethoxy]carbonyl]amino]-1,3-butadiene (21).** This compound was prepared according to the procedure of L. Overman and co-workers<sup>37</sup> with 2-(trimethylsilyl)ethanol in place of benzyl alcohol. The product was purified by flash chromatography on silica gel using 7.5% EtOAc/hexanes to give **21** (59.7 g, 56%) as a white solid: <sup>1</sup>H NMR (400 MHz, CDCl<sub>3</sub>)  $\delta$  6.75 (app t, 1,  $J$  = 12.5), 6.50 (br s, 1), 6.27 (dt, 1,  $J$  = 10.3, 16.8), 5.69 (app t, 1,  $J$  = 12.2), 5.02 (d, 1,  $J$  = 16.9), 4.90 (d, 1,  $J$  = 10.3), 4.22 (t, 2,  $J$  = 8.3), 1.00 (t, 2,  $J$  = 8.2), 0.05 (s, 9); <sup>13</sup>C NMR (100 MHz, CDCl<sub>3</sub>)  $\delta$  153.6, 134.5, 127.2, 113.1, 111.6, 63.9, 17.7, -1.5. Anal. Calcd for C<sub>10</sub>H<sub>19</sub>NO<sub>2</sub>Si: C, 56.30; H, 8.98; N, 6.57. Found: C, 56.40; H, 9.19; N, 6.44.

**Ethyl 2-[[[2-(Trimethylsilyl)ethoxy]carbonyl]amino]cyclohexa-1,4-diene-1-carboxylate (22).** Diene **21** (10.0 g, 46.9 mmol) and ethyl propiolate (11.5 g, 11.9 mL, 117.2 mmol) were combined in a 250-mL round-bottomed flask equipped with a reflux condenser. The mixture was heated under an atmosphere of argon at 85 °C in an oil bath for 48 h. The reaction mixture was cooled to room temperature, diluted with a small amount of hexanes, and purified by flash chromatography with a gradient of 10–15% EtOAc/hexanes to give **22** (13.0 g, 89%) as a pale yellow solid: <sup>1</sup>H NMR (400 MHz, CDCl<sub>3</sub>)  $\delta$  7.14 (s, 1), 5.85 (s, 2), 5.10 (m, 1), 4.61 (br s, 1), 4.30–4.10 (m, 4), 2.76–2.96 (m, 2), 1.28 (t, 3,  $J$  = 7.1), 0.97 (t, 2,  $J$  = 8.2), 0.03 (s, 9); <sup>13</sup>C NMR (100 MHz, CDCl<sub>3</sub>)  $\delta$  166.0, 155.7, 139.2, 129.1, 126.5, 124.4, 63.0, 60.6, 43.8, 27.1, 17.7, 14.2, -1.5; HRMS-FAB (MH<sup>+</sup>) calcd 312.1631, found 312.1634. Anal. Calcd for C<sub>15</sub>H<sub>25</sub>NO<sub>4</sub>Si: C, 57.85; H, 8.09; N, 4.50. Found: C, 57.61; H, 8.14; N, 4.51.

**Ethyl (5R\*,6R\*)-5-Hydroxy-6-[[[2-(trimethylsilyl)ethoxy]carbonyl]amino]cyclohexa-1,3-dienecarboxylate (25).** Diene **22** (25.0

g, 80.3 mmol), NaHCO<sub>3</sub> (16.9 g, 200.7 mmol), and CH<sub>2</sub>Cl<sub>2</sub> (600 mL) were combined and heated at reflux in a 2-L three-necked round-bottom flask equipped with a pressure-equalizing addition funnel and a reflux condenser. A solution of *m*-CPBA (26.0 g, 120.4 mmol, 85% pure) dissolved in 350 mL of CH<sub>2</sub>Cl<sub>2</sub> was added dropwise to the reaction mixture over 45 min. This mixture was heated at reflux for an additional 4 h, cooled to room temperature, and allowed to stir overnight. The mixture was cooled in an ice bath, and 10% aqueous NaHSO<sub>3</sub> was added until starch/KI test paper indicated that all of the excess *m*-CPBA was consumed. The organic layer was isolated, washed with 1:1 saturated Na<sub>2</sub>CO<sub>3</sub>/H<sub>2</sub>O (2 × 400 mL) and brine (300 mL), and dried over MgSO<sub>4</sub>, and the volume of the solution was reduced to 250 mL by rotary evaporation at aspirator pressure.

To the solution of crude epoxides **23** and **24** was added DBU (24.4 g, 24.0 mL, 160.5 mmol), and the mixture was stirred at room temperature for 3 h. The solvent was removed, the residue was dissolved in 500 mL of EtOAc, and the solution was washed with 1:1 saturated NaHCO<sub>3</sub>/H<sub>2</sub>O (2 × 400 mL), 1:1 saturated Na<sub>2</sub>CO<sub>3</sub>/H<sub>2</sub>O (300 mL), H<sub>2</sub>O (350 mL), and brine (200 mL), dried over MgSO<sub>4</sub>, and evaporated. The crude alcohol was purified by flash chromatography using 35% EtOAc/hexanes to give **25** (9.50 g, 36%): <sup>1</sup>H NMR (400 MHz, CDCl<sub>3</sub>)  $\delta$  7.19 (d, 1,  $J$  = 4.8), 6.29 (m, 2), 4.82 (dd, 1,  $J$  = 2.3, 8.1), 4.65 (br d, 1,  $J$  = 6.7), 4.35 (br s, 1), 4.19–4.29 (m, 2), 4.14 (t, 2,  $J$  = 7.8), 3.30 (br m, 1), 1.29 (t, 3,  $J$  = 7.1), 0.95 (t, 2,  $J$  = 7.8), 0.03 (s, 9); <sup>13</sup>C NMR (100 MHz, CDCl<sub>3</sub>)  $\delta$  165.8, 156.3, 133.6, 132.7, 127.0, 124.4, 67.5, 63.4, 60.8, 50.1, 17.6, 14.1, -1.6; HRMS-FAB (MH<sup>+</sup>) calcd for C<sub>15</sub>H<sub>26</sub>NO<sub>5</sub>Si 328.1580, found 328.1581.

**Ethyl (1R\*,4S\*,5S\*,6R\*)-5-[Bis(methoxycarbonyl)methoxy]-4-[[[2-(trimethylsilyl)ethoxy]carbonyl]amino]-7-oxabicyclo[4.1.0]hept-2-ene-3-carboxylate (26).** Alcohol **25** (9.50 g, 29.1 mmol), dimethyl diazomalonate (5.50 g, 34.8 mmol), Rh<sub>2</sub>(OAc)<sub>4</sub> (0.26 g, 0.58 mmol), and benzene (200 mL) were combined, and the mixture was heated at 70 °C under an atmosphere of nitrogen. After 1 h, more dimethyl diazomalonate (1.60 g, 10.1 mmol) was added and heating was continued for an additional 1 h. The reaction mixture was cooled to room temperature, and the solution was filtered to remove the catalyst. The solvent was removed, and the crude material was purified by flash chromatography using 25% EtOAc/hexanes to give the malonyl ether (7.18 g, 54%): <sup>1</sup>H NMR (400 MHz, CDCl<sub>3</sub>)  $\delta$  7.14 (d, 1,  $J$  = 5.6), 6.31–6.20 (m, 2), 5.02 (s, 1), 4.79 (d, 1,  $J$  = 7.3), 4.54 (d, 1,  $J$  = 7.1), 4.04–4.20 (m, 4), 3.75 (m, 1), 3.73 (s, 3), 1.22 (t, 3,  $J$  = 7.1), 0.87 (t, 2,  $J$  = 8.3), -0.05 (s, 9); <sup>13</sup>C NMR (100 MHz, CDCl<sub>3</sub>)  $\delta$  167.3, 166.3, 165.2, 155.87, 133.6, 128.9, 126.7, 126.0, 75.4, 63.2, 60.7, 52.7, 46.6, 17.4, 14.0, -1.7; HRMS-FAB (M<sup>+</sup>) calcd for C<sub>20</sub>H<sub>31</sub>NO<sub>5</sub>Si 457.1768, found 457.1764.

The malonyl ether (6.86 g, 15.0 mmol), NaHCO<sub>3</sub> (3.15 g, 37.5 mmol), *m*-CPBA (4.85 g, 22.5 mmol, 85% pure), and CH<sub>2</sub>Cl<sub>2</sub> (100 mL) were combined in a flask equipped with a reflux condenser, and the mixture was heated at 60 °C in an oil bath for 5 h. The reaction mixture was cooled to room temperature, and the solvent was removed. The residue was taken up in 400 mL of EtOAc, and the organic layer was washed with H<sub>2</sub>O (300 mL), 10% aqueous NaHSO<sub>3</sub> (300 mL), saturated aqueous NaHCO<sub>3</sub> (300 mL), H<sub>2</sub>O (300 mL), and brine (300 mL) and dried over MgSO<sub>4</sub>, and the solvent was removed by rotary evaporation at aspirator pressure. The crude material was purified by flash chromatography using 30% EtOAc/hexanes to give epoxide **26** (4.82 g, 68%): <sup>1</sup>H NMR (500 MHz, CDCl<sub>3</sub>)  $\delta$  7.34 (d, 1,  $J$  = 4.2), 4.97 (d, 1,  $J$  = 9.6), 4.87 (s, 1), 4.70 (d, 1,  $J$  = 9.6), 4.20–4.27 (m, 2), 4.08–4.18 (m, 3), 3.94 (m, 1), 3.84 (s, 3), 3.78 (s, 3), 3.58 (t, 1,  $J$  = 4.0), 1.30 (t, 3,  $J$  = 7.1), 0.96 (t, 2,  $J$  = 8.5), 0.03 (s, 9); <sup>13</sup>C NMR (125 MHz, CDCl<sub>3</sub>)  $\delta$  166.9, 165.9, 164.4, 155.5, 137.1, 131.9, 77.9, 75.6, 63.2, 61.1, 60.2, 56.2, 52.9, 46.2, 45.9, 17.5, 14.0, -1.7; HRMS-FAB (MH<sup>+</sup>) calcd 474.1796, found 474.1789. Anal. Calcd for C<sub>20</sub>H<sub>32</sub>NO<sub>10</sub>Si: C, 50.73; H, 6.60; N, 2.96. Found: C, 50.44; H, 6.52; N, 2.93.

**Ethyl (4S\*,5R\*,6R\*)-4-Hydroxy-5-[bis(methoxycarbonyl)methoxy]-6-[[[2-(trimethylsilyl)ethoxy]carbonyl]amino]cyclohex-1-enecarboxylate (27).** Epoxide **26** (0.766 g, 1.62 mmol) and benzeneselenol (1.02 g, 0.687 mL, 6.47 mmol) were combined in a 25-mL round-bottomed flask equipped with a reflux condenser. The reaction mixture was heated in a 60 °C oil bath under an atmosphere of argon for 4 h and cooled to room temperature, and the material was purified by flash

chromatography using 2% MeOH/CH<sub>2</sub>Cl<sub>2</sub> to give **27** (0.66 g, 85%): <sup>1</sup>H NMR (400 MHz, CDCl<sub>3</sub>) δ 6.88 (s, 1), 5.21 (br s, 1), 4.80 (s, 1), 4.40 (br s, 1), 3.98–4.19 (m, 6), 3.86 (br s, 1), 3.78 (s, 3), 3.76 (s, 3), 2.65 (dt, 1, *J* = 4.5, 18.7), 2.30 (m, 1), 1.22 (t, 3, *J* = 7.1), 0.92 (m, 2), –0.01 (s, 9); <sup>13</sup>C NMR (100 MHz, CDCl<sub>3</sub>) δ 168.2, 166.5, 165.3, 156.0, 138.0, 129.2, 84.6, 79.4, 67.1, 63.0, 60.6, 53.1, 52.9, 51.2, 31.2, 17.6, 14.0, –1.6; HRMS-FAB (MH<sup>+</sup>) calcd for C<sub>20</sub>H<sub>34</sub>NO<sub>10</sub>Si 476.1952, found 476.1968.

**Ethyl (4*S*\*,5*R*\*,6*R*\*)-4-(*tert*-Butyldimethylsiloxy)-5-[[1-(methoxycarbonyl)ethenyl]oxy]-6-[[[2-(trimethylsilyl)ethoxy]carbonyl]amino]-cyclohex-1-enecarboxylate (**28**).** Alcohol **27** (0.66 g, 1.38 mmol) was dissolved in CH<sub>2</sub>Cl<sub>2</sub> (15 mL), and the solution was cooled in an ice bath under an atmosphere of nitrogen. Collidine (0.33 g, 0.37 mL, 2.76 mmol) and then *tert*-butyldimethylsilyl triflate (TBDMSOTf) (0.47 g, 0.41 mL, 1.80 mmol) were added dropwise to the reaction mixture via syringe. After the additions were complete, the mixture was allowed to stir at 0 °C for 30 min. The cold reaction mixture was poured into 100 mL of EtOAc, and the organic layer was washed with 0.1 N aqueous HCl (3 × 75 mL), H<sub>2</sub>O (100 mL), saturated aqueous NaHCO<sub>3</sub> (100 mL), H<sub>2</sub>O (100 mL), and brine (50 mL) and dried over MgSO<sub>4</sub>. After removal of the solvent, the crude product was purified by flash chromatography using 15% EtOAc/hexanes to give the silyl ether (0.69 g, 85%): <sup>1</sup>H NMR (400 MHz, CDCl<sub>3</sub>) δ 7.04 (app d, 1, *J* = 2.6), 5.05 (d, 1, *J* = 9.9), 4.88 (s, 1), 4.67 (d, 1, *J* = 9.9), 4.32 (br s, 1), 4.10–4.28 (m, 4), 3.81 (s, 3), 3.78 (s, 3), 3.71 (m, 1), 2.68 (app br d, 1, *J* = 19.5), 2.28 (ddd, 1, *J* = 1.6, 5.2, 19.5), 1.28 (t, 3, *J* = 7.3), 0.93 (m, 2), 0.88 (s, 6), 0.09 (m, 9), 0.02 (s, 9); <sup>13</sup>C NMR (100 MHz, CDCl<sub>3</sub>) δ 167.3, 166.3, 165.8, 155.7, 138.7, 127.3, 79.0, 77.5, 66.1, 62.9, 60.5, 52.9, 45.4, 30.5, 25.8, 21.0, 18.0, 17.6, 14.1, –1.5, –5.1; HRMS-FAB (MH<sup>+</sup>) calcd for C<sub>26</sub>H<sub>48</sub>NO<sub>10</sub>Si<sub>2</sub> 590.2817, found 590.2823.

The silyl ether (1.86 g, 3.15 mmol), *N,N*-dimethylmethyleammonium iodide (0.87 g, 4.73 mmol), Et<sub>3</sub>N (0.64 g, 0.88 mL, 6.30 mmol), and CH<sub>2</sub>Cl<sub>2</sub> (30 mL) were combined in a 100-mL round-bottomed flask, and the solution was stirred at room temperature for 2 h under an atmosphere of nitrogen. The solution was diluted with 250 mL of EtOAc, washed with H<sub>2</sub>O (200 mL), 1:1 saturated aqueous Na<sub>2</sub>CO<sub>3</sub>/H<sub>2</sub>O (200 mL), H<sub>2</sub>O (200 mL), and brine (100 mL), and dried over MgSO<sub>4</sub>, and the solvent was removed.

Methyl iodide (5 mL) was added to a solution of the crude Mannich base in dry acetonitrile (40 mL). The solution was heated in an oil bath under an atmosphere of nitrogen for at 50 °C for 3 h and then at 100 °C for 36 h. The reaction was cooled to room temperature, the solvent was removed, and the residue was dissolved in 200 mL of EtOAc. The organic layer was washed with H<sub>2</sub>O (200 mL), 1:1 saturated aqueous Na<sub>2</sub>CO<sub>3</sub>/H<sub>2</sub>O (200 mL), H<sub>2</sub>O (200 mL), and brine (100 mL) and dried over MgSO<sub>4</sub>, and the solvent was removed. The crude material was purified by flash chromatography using 15% EtOAc/hexanes to give enolpyruvyl ether **28** (1.21 g, 71%): <sup>1</sup>H NMR (400 MHz, CDCl<sub>3</sub>) δ 7.07 (app d, 1, *J* = 2.9), 5.56 (d, 1, *J* = 3.2), 5.30 (d, 1, *J* = 3.1), 5.10 (d, 1, *J* = 10.1), 4.87 (d, 1, *J* = 10.1), 4.09–4.27 (m, 5), 3.76 (s, 3), 2.73 (br d, 1, *J* = 19.5), 2.32 (dd, 1, *J* = 5.3, 19.6), 1.27 (t, 3, *J* = 7.1), 0.95 (m, 2), 0.89 (s, 6), 0.10 (s, 9), 0.03 (s, 9); <sup>13</sup>C NMR (100 MHz, CDCl<sub>3</sub>) δ 165.7, 163.1, 155.8, 148.8, 138.4, 127.6, 97.8, 75.7, 65.8, 63.0, 60.6, 52.3, 43.07, 30.7, 25.8, 18.0, 17.6, 14.1, –1.5, –5.0; HRMS-FAB (MH<sup>+</sup>) calcd for C<sub>25</sub>H<sub>46</sub>NO<sub>8</sub>Si<sub>2</sub> 544.2762, found 544.2742.

**NMR Spectroscopy of Compounds 1–3.** Compounds **1–3** were dissolved in D<sub>2</sub>O to give approximately 70–75 mM solutions. The pH was adjusted with DCl or NaOD to pH 7.8 for compounds **1** and **2** and pH 8.2 for compound **3**. <sup>1</sup>H NMR spectra were recorded on a Bruker AMX-300 spectrometer from 278 to 363 K at 5-K increments. The FIDs were resolution enhanced using Gaussian multiplication and negative line broadening prior to Fourier transformation. The axial–equatorial equilibria for these materials, as indicated in Table 2, were calculated according to eq 1 and depend on the limiting values chosen for *J*<sub>AX</sub> and *J*<sub>EQ</sub>.

**Enzyme Assays, General.** Isochorismate synthase (IS) and isochorismatase were provided by Prof. Christopher T. Walsh (Harvard Medical School), anthranilate synthase (AS) by Prof. Nicholas Amrhein (ETH Zürich), *p*-aminobenzoate synthase (PABS) by Prof. Brian P. Nichols (University of Illinois at Chicago), chorismate mutase/prephenate dehydrogenase from *E. coli* JFM-30 by Prof. Jeremy

Knowles (Harvard University), and ADIC by Prof. Ronald Bauerle (University of Virginia). Lactate dehydrogenase (rabbit muscle type XI) and chorismate were obtained from Sigma. NADH was obtained from Boehringer-Mannheim. *N*-Ethylmorpholine was distilled from Na prior to use. All solutions were prepared using doubly distilled deionized water and were 0.45-μm filtered.

The concentrations of chorismate solutions were determined spectrophotometrically from ε<sub>273</sub> = 2630 M<sup>-1</sup> cm<sup>-1</sup>.<sup>61</sup> Since compounds **1–3** exist as hydrates, the purities of their sodium salts were calculated on the basis of the %C found by combustion analysis. The concentrations of aqueous solutions of inhibitors **1–3** were also determined by treating an aliquot with 0.4 M HCl at 100 °C for 30 min and assaying the released pyruvate with LDH, monitoring the total amount of NADH oxidized (ε<sub>340</sub> = 6220 M<sup>-1</sup> cm<sup>-1</sup>). Inhibitor solutions were brought to pH 12 with NaOH for storage to prevent hydrolysis of the enolpyruvyl side chain.

**Isochorismate Synthase Assays.**<sup>13</sup> All assays were performed at 37 °C on a Kontron Uvikon 860 UV–vis spectrophotometer. The forward reaction rate was measured by monitoring the absorbance change at 275 nm in a coupled assay with excess isochorismatase. The initial rate was calculated on the basis of the extinction coefficients of the substrate (chorismate, λ<sub>max</sub> = 273 nm, ε<sub>1</sub> = 2630 M<sup>-1</sup> cm<sup>-1</sup>) and the product (2,3-dihydro-2,3-dihydroxybenzoate, λ<sub>max</sub> = 278 nm, ε<sub>2</sub> = 8150 M<sup>-1</sup> cm<sup>-1</sup>) according to eq 2.

$$A = \frac{\Delta A}{\Delta t} \frac{10^6}{\epsilon_1 - \epsilon_2} = \frac{\Delta A}{\Delta t} \frac{10^6}{5520} \quad (\mu\text{M min}^{-1}) \quad (2)$$

Enzyme dilutions were made with buffer containing 100 mM Tris-HCl (pH 7.8), 10 mM MgCl<sub>2</sub>, and 20% (v/v) glycerol. The assay mixture contained 100 mM Tris-HCl (pH 7.8) and 10 mM MgCl<sub>2</sub>, and the total volume for all assays was 1.00 mL. The reaction was initiated with IS. For each inhibitor concentration examined (compound **1**: 0, 0.5, 1, 5, and 10 μM; compound **2**: 0, 0.05, 0.1, 0.2, and 0.4 μM; compound **3**: 0, 0.08, 0.24, 0.80, and 2.40 μM), five substrate concentrations were used (4, 8, 14, 20, and 30 μM) with two independent determinations at each concentration. Initial rates were calculated using the ENZFITTER program.<sup>62</sup> All measured rates were corrected for a small background rate observed when the assay was run without isochorismate synthase. A reciprocal plot of these data clearly indicated competitive inhibition. *K<sub>i</sub>* and *K<sub>m</sub>* values were determined by fitting the data to the equation  $Y = VA/(K(1 + I/K_i) + A)$  with Cleland's COMPO program.<sup>63</sup>

Doubling the amount of IS resulted in a doubling of the rate in assays with or without inhibitor, indicating that the isochorismatase reaction was properly coupled. A further series of control reactions was performed for compound **1**. Incubation of this material in the presence of IS did not produce any spectrophotometrically detectable amount of either chorismate or isochorismate, which confirms that the inhibitor was not a substrate for IS. Incubation of **1** in the presence of IS, isochorismatase, LDH, and NADH (0.2 mM) did not lead to any consumption of NADH (as measured at 340 nm), which indicates that the enolpyruvyl side chain of inhibitor **1** is not hydrolyzed by isochorismatase under standard assay conditions. Finally, changing the concentration of the coupling enzyme, with or without **1**, did not alter the observed rate, which implies that compound **1** does not inhibit isochorismatase significantly.

**Anthranilate Synthase Assays.**<sup>44</sup> All assays were performed at 22 °C using a PTI spectrofluorimeter to measure anthranilate formation. The sample was excited at 325 nm, and emission was monitored at 400 nm with 3-nm slit widths. Enzyme dilutions were made with buffer containing 50 mM potassium phosphate (pH 7.6), 0.1 mM ethylenediaminetetraacetic acid (EDTA), 0.2 mM dithiothreitol (DTT), and 5 mg/mL bovine serum albumin (BSA). The assay mixture contained 50 mM potassium phosphate (pH 7.5), 10 mM MgCl<sub>2</sub>, and 5 mM glutamine, and the total volume for all assays was 0.50 mL. The reaction was initiated with anthranilate synthase.

(61) Heyde, E.; Morrison, J. F. *Biochemistry* **1978**, *17*, 1573–1580.

(62) Leatherbarrow, R. J. *ENZFITTER*; Elsevier Science Publishers BV: Amsterdam, 1987.

(63) Cleland, W. W. *Methods Enzymol.* **1979**, *63*, 103–138.

For each inhibitor concentration examined (compound 1: 0, 10, 50, 100, 500  $\mu\text{M}$ ; compound 2: 0, 0.5, 1, 5, and 10  $\mu\text{M}$ ; compound 3: 0, 0.8, 8, 24, and 80  $\mu\text{M}$ ), five substrate concentrations were used (2, 5, 10, 20, and 30  $\mu\text{M}$ ) with two independent determinations at each concentration. Initial rates were calculated using the Alpha program (PTI). All rates measured were corrected for a small background rate observed when the assay was run without anthranilate synthase. A reciprocal plot of these data clearly indicated competitive inhibition.  $K_i$  and  $K_m$  values were determined by fitting the data to the equation  $Y = VA/(K(1 + I/K_i) + A)$  with Cleland's COMPO program.<sup>63</sup>

***p*-Aminobenzoate Synthase Assays.**<sup>21</sup> All assays were performed at 37 °C on a Kontron Uvikon 860 UV-vis spectrophotometer. The forward reaction rate was measured by following the formation of pyruvate by the consumption of NADH ( $\epsilon = 6220$  at 340 nm) in a coupled assay with excess LDH. PABS-II was diluted with 50 mM Tris-HCl (pH 7.8), 5 mM MgCl<sub>2</sub>, 1 mM EDTA, 10 mM DTT, and 5 mg/mL BSA. PABS-I and PABS-III were diluted with 50 mM Tris-HCl (pH 7.8), 5 mM MgCl<sub>2</sub>, 1 mM EDTA, and 5 mg/mL BSA. A ratio of 1 unit:5 units:6 units of PABS-I:PABS-II:PABS-III was the smallest excess of coupling enzymes that provided a satisfactorily coupled reaction. The assays were carried out in a buffer containing 50 mM Tris-HCl (pH 7.8), 5 mM MgCl<sub>2</sub>, 5 mM glutamine, 0.2 mM NADH, and 50  $\mu\text{g/mL}$  LDH; the total volume for all assays was 1.00 mL. The assay mixture was equilibrated for 4 min at 37 °C prior to initiation of the reaction with substrate.

A full kinetic analysis was carried out for inhibitors 1 and 3. At each concentration examined (compound 1: 100, 250, and 500  $\mu\text{M}$ ; compound 3: 0, 10, 100, and 210  $\mu\text{M}$ ), four substrate concentrations were used (5, 10, 20, and 30  $\mu\text{M}$ ) with two independent determinations at each concentration. Initial rates were calculated using the ENZFITTER program.<sup>62</sup> All rates measured were corrected for a background rate observed when the assay was run without substrate. A reciprocal plot of these data clearly indicated competitive inhibition.  $K_i$  and  $K_m$  values were determined by fitting the data to the equation  $Y = VA/(K(1 + I/K_i) + A)$  with Cleland's COMPO program.<sup>63</sup>

For compound 2,  $K_i$  was calculated by a Dixon analysis. Several inhibitor concentrations were examined with substrate concentration equal to  $\sim 2K_m$  (5  $\mu\text{M}$ ). Initial rates were calculated using the ENZFITTER program. All rates measured were corrected for a background rate observed in the absence of substrate. Competitive inhibition was assumed, and  $K_i$  was calculated with ENZFITTER using the equation  $V_o/V_i = ([I]/K_i)\{K_m/(K_m + [S])\} + 1$ .

**Chorismate Mutase Assays.**<sup>46,47</sup> The enzyme used for the assays was chorismate mutase/prephenate dehydrogenase (T-protein) from *E. coli* JFM-30; it had been purified by ammonium sulfate fractionation and stored at -78 °C. Concentrated enzyme was in a stabilizing buffer containing 0.1 M *N*-ethylmorpholine (NEM), 1 mM dithioerythritol (DTE), 21 mM trisodium citrate, 1 mM EDTA, and 10% (v/v) glycerol, adjusted to pH 7.0 with concentrated HCl. Prior to the assay, stock enzyme solutions were allowed to reactivate at 0 °C for 2 h. The assays were carried out in buffer containing 50 mM NEM, 0.5 mM DTE, 1.0 mM trisodium citrate, 0.1 mg/mL BSA, and 10% (v/v) glycerol adjusted to pH 7.5 with concentrated HCl; the total volume for all assays was 1.00 mL.

Assays were performed at 30 °C on a Kontron Uvikon 860 UV-vis spectrophotometer. The conversion of chorismate to prephenate was monitored directly by observing the disappearance of chorismate at 274 nm ( $\epsilon_1 = 2630 \text{ M}^{-1} \text{ cm}^{-1}$ ).<sup>61</sup> The reaction was initiated with chorismate mutase.  $K_m$  values were determined over a range of substrate concentrations (5, 10, 20, 50, 100, and 200  $\mu\text{M}$ ). Several inhibitor concentrations were examined while the substrate concentration was kept equal to  $K_m$  (31.6  $\mu\text{M}$ ). Initial rates were calculated using the ENZFITTER program.<sup>62</sup> The rates measured were not corrected for any background rate observed when the assay was performed without chorismate mutase, since this rate was negligible. Competitive inhibition was assumed, and  $K_i$  was calculated by a Dixon analysis performed with ENZFITTER according to the equation  $V_o/V_i = ([I]/K_i)\{K_m/(K_m + [S])\} + 1$ .

**IS HPLC Assays.** The rates of chorismate disappearance, ADIC formation,<sup>17</sup> and isochorismate formation were determined by HPLC.

Since the rate of isochorismate formation is fast relative to that of ADIC, this rate was also measured with the isochorismatase-coupled UV assay.<sup>13</sup>

All HPLC studies were performed on an HP series 1050 HPLC with an HP 3396A integrator. An analytical Vydac Proteins and Peptides (25 cm  $\times$  4.6 mm) 10- $\mu\text{m}$  C<sub>18</sub> reverse phase column was used; peaks were detected at 280 nm. Solvent A was 0.1% aqueous TFA and solvent B was 0.1% TFA in acetonitrile. The following gradient was used for all runs: 0 min, 5% B; 2 min, 5% B; 17 min, 50% B; 19 min, 50% B; 21 min, 100% B; 30 min, 100% B; 31 min, 5% B; 40 min, 5% B (at 1 mL/min). Each 500  $\mu\text{L}$  injection consisted of 100  $\mu\text{L}$  of the assay mixture or standard solution mixed with 400  $\mu\text{L}$  of solvent A. This sequence prevented the sample solvent or buffer from affecting the chromatographic separation, thereby ensuring uniform peak shapes and retention times. The following retention times were observed with this protocol: ADIC ( $\epsilon_{280} = 11\,500 \text{ M}^{-1} \text{ cm}^{-1}$ ),<sup>17</sup>  $T_R = 7.5$  min; isochorismate ( $\epsilon_{280} = 12\,800 \text{ M}^{-1} \text{ cm}^{-1}$ ),<sup>14</sup>  $T_R = 9.1$  min; chorismate ( $\epsilon_{280} = 2630 \text{ M}^{-1} \text{ cm}^{-1}$ ),<sup>61</sup>  $T_R = 9.9$  min; anthranilate ( $\epsilon_{280} = 2000 \text{ M}^{-1} \text{ cm}^{-1}$ ),  $T_R = 10.0$  min; *p*-hydroxybenzoate (an impurity in commercial chorismate preparations),<sup>17</sup>  $T_R = 10.4$  min. Prephenate did not produce any significant peak at this wavelength.

All assay solutions were maintained at 37 °C using a Lauda Model RM 20 circulating bath. Enzyme dilutions were made with buffer containing 100 mM Tris-HCl (pH 7.8), 10 mM MgCl<sub>2</sub>, and 20% (v/v) glycerol. The assay was performed in either buffer A (without ammonia) containing 100 mM Tris-HCl (pH 7.8) and 10 mM MgCl<sub>2</sub> or buffer B (with ammonia) containing 100 mM Tris-HCl (pH 8.0), 10 mM MgCl<sub>2</sub>, and 50 mM (NH<sub>4</sub>)<sub>2</sub>SO<sub>4</sub>. The total volume for all assays was 0.5 mL, and the reaction was initiated with substrate.

**HPLC.** Reaction mixtures were comprised of IS and 30  $\mu\text{M}$  chorismate in buffer B. Aliquots were analyzed by HPLC at various times (0–480 min) during the course of the reaction. The concentrations of ADIC, isochorismate, and chorismate were determined from the integration values according to their respective extinction coefficients and normalization of the sum of their concentrations to 30  $\mu\text{M}$  to correct for any decomposition of chorismate. The percent decomposition for each run was determined by comparing the crude summed concentrations after correcting for differing injection volumes using the *p*-hydroxybenzoate standard. The concentration of ADIC was plotted vs time, and an initial rate for ADIC formation was computed with the ENZFITTER<sup>62</sup> program using the linear portion of the curve. The rates of isochorismate formation and chorismate disappearance were too rapid to be quantitated in this manner.

**UV.** The rate of isochorismate formation was determined on a Kontron Uvikon 860 UV-vis spectrophotometer at 275 nm, as described above. Initial rates were calculated using the ENZFITTER program.<sup>62</sup> The assay mixture consisted of 30  $\mu\text{M}$  chorismate, IS, and isochorismatase in buffer A or B. The formation of isochorismate was found to be 25% slower in the presence of ammonia. Proper coupling with isochorismatase was verified for buffers A and B either by halving the amount of IS used (which gave one-half the rate) or by doubling the amount of isochorismatase used (which gave the same rate).

**Fluorimetry.** To determine whether anthranilate was formed by contaminating AS, samples were monitored with a PTI fluorimeter. The sample was excited at 325 nm, and emission was monitored at 400 nm with 3-nm slit widths used throughout. The initial rates were calculated from the linear portion of a plot of fluorescence vs time with the Alpha program (PTI). Rates were converted to  $\mu\text{M/min}$  using an anthranilate fluorescence calibration curve generated with stock solutions of anthranilate (0–0.025  $\mu\text{M}$ ). The assay mixture consisted of 30  $\mu\text{M}$  chorismate and IS in buffer A or B. The rates were corrected for background when the assay was performed without substrate. Small, positive changes in fluorescence were observed in both buffers A and B, although the rate was lower for buffer A.

**Acknowledgment.** We express our appreciation to the many individuals and groups who have generously provided us with enzymes: Prof. Christopher T. Walsh (Harvard Medical School, isochorismate synthase and isochorismatase), Prof. Nicholas Amrhein (ETH Zürich, anthranilate synthase), Prof. Brian P. Nichols (University of Illinois at Chicago, *p*-aminobenzoate

synthase), Prof. Jeremy R. Knowles (Harvard University, chorismate mutase), and Prof. Ronald Bauerle (University of Virginia, for the kind gift of ADIC). We also thank Chris Walsh for discussions that led to the initiation of this project, Anthony A. Morollo (University of Virginia) for helpful discussions regarding AS, Matthew Marx for providing samples of the rigid compounds of Scheme 8, and Mark Hediger for suggesting benzeneselenol reduction of epoxide **26**. This work was supported by the National Institutes of Health (Grant No. GM-28965) and by a Syntex fellowship to M.C.K.

**Supplementary Material Available:** Figures showing  $^1\text{H}$  NMR and  $^{13}\text{C}$  NMR characterizations for compound **2**, temperature dependences of  $J$  values for **1**, **2**, and **3**, and kinetic plots for determination of  $K_i$  values (4 pages). This material is contained in many libraries on microfiche, immediately follows this article in the microfilm version of the journal, and can be ordered from the ACS; see any current masthead page for ordering information.

JA942245F